EARTH SURFACE PROCESSES AND LANDFORMS
Earth Surf. Process. Landforms **45**, 2647–2663 (2020)

Published online 4 July 2020 in Wiley Online Library
(wileyonlinelibrary.com) DOI: 10.1002/esp.4920

Long-term impact of the proglacial lake Jökulsárlón on the flow velocity and stability of Breiðamerkurjökull glacier, Iceland

Nathaniel R. Baurley,[1]* Benjamin A. Robson[2] and Jane K. Hart[1]
[1] Geography and Environmental Science, University of Southampton, Southampton SO17 1BJ, UK
[2] Department of Geography, University of Bergen, Bergen 5007, Norway

Received 12 December 2019; Revised 18 May 2020; Accepted 19 May 2020

*Correspondence to: Nathaniel R. Baurley, Geography and Environmental Science, University of Southampton, Southampton SO17 1BJ, UK.
E-mail: nrb1n18@soton.ac.uk

ESPL
Earth Surface Processes and Landforms

ABSTRACT: Proglacial lakes are becoming ubiquitous at the termini of many glaciers worldwide due to continued climate warming and glacier retreat, and such lakes have important consequences for the dynamics and future stability of these glaciers. In light of this, we quantified decadal changes in glacier velocity since 1991 using satellite remote sensing for Breiðamerkurjökull, a large lake-terminating glacier in Iceland. We investigated its frontal retreat, lake area change and ice surface elevation change, combined with bed topography data, to understand its recent rapid retreat and future stability. We observed highly spatially variable velocity change from 1991 to 2015, with a substantial increase in peak velocity observed at the terminus of the lake-terminating eastern arm from ~1.00±0.36 m day^{-1} in 1991 to 3.50±0.25 m day^{-1} in 2015, with mean velocities remaining elevated from 2008 onwards. This is in stark comparison to the predominately land-terminating arms, which saw no discernible change in their velocity over the same period. We also observed a substantial increase in the area of the main proglacial lake (Jökulsárlón) since 1982 of ~20 km^2, equating to an annual growth rate of 0.55 km^2 year^{-1}. Over the same period, the eastern arm retreated by ~3.50 km, which is significantly greater than the other arms. Such discrepancies between the different arms are due to the growth and, importantly, depth increase of Jökulsárlón, as the eastern arm has retreated into its ~300 m-deep reverse-sloping subglacial trough. We suggest that this growth in lake area, forced initially by rising air temperatures, combined with the increase in lake depth, triggered an increase in flow acceleration, leading to further rapid retreat and the initiation of a positive feedback mechanism. These findings may have important implications for how increased melt and calving forced by climate change will affect the future stability of large soft-bedded, reverse-sloped, subaqueous-terminating glaciers elsewhere. © 2020 The Authors. Earth Surface Processes and Landforms published by John Wiley & Sons Ltd

KEYWORDS: glacier dynamics; velocity; retreat; proglacial Lakes; calving; remote sensing

Introduction

Continued and more intensive global climate warming, particularly over the last decade, is driving patterns of glacier recession and dynamics, and consequently it is now widely established that almost all glaciers worldwide are undergoing widespread retreat (Björnsson *et al.*, 2013; Zemp *et al.*, 2015; Glasser *et al.*, 2016). This has important consequences for their meltwater contribution to global sea level rise (s.l.r.) (Huss and Hock, 2015; Cazenave and WCRP Global Sea Level Budget Group, 2018; Rossini *et al.*, 2018; Zemp *et al.*, 2019), as well as for regional hydrology due to the strong control glacier meltwater has on modulating down-glacier streamflow, which in turn affects freshwater availability, hydropower operations and sediment transport (Immerzeel *et al.*, 2014; Huss and Hock, 2018; Shannon *et al.*, 2019).

There are several different mechanisms which it is believed are causing the widely observed dynamic changes occurring at land-, lake- and marine-terminating outlet glaciers. For example, some land-terminating glaciers globally are slowing down due to a reduction in ice thickness and surface slope, which has caused a corresponding decrease in the driving stress, and consequently ice flow over recent decades (Heid and Kääb, 2012; Mernild *et al.*, 2013; Dehecq *et al.*, 2019). In contrast, increased surface melt may lead to increased seasonal velocities, via basal lubrication and till deformation (e.g. Boulton *et al.*, 2001; Zwally *et al.*, 2002; Schoof, 2010;

Bartholomew *et al.*, 2011; Hart *et al.*, 2011; Andrews *et al.*, 2014; Bougamont *et al.*, 2014; Hart *et al.*, 2019a). This process can vary considerably over the melt season, however, depending on several different factors (Bartholomew *et al.*, 2012; Tedstone *et al.*, 2013; Hart *et al.*, 2019b). These include: (i) the nature of the basal drainage system in place (e.g. inefficient cavities vs. efficient channels) (Röthilsberger, 1972; Schoof, 2010); (ii) both the amount and the rate at which meltwater reaches the bed (Meierbachtol *et al.*, 2013; Sole *et al.*, 2013); and (iii) the area covered by one of these drainage systems at the expense of the other, and the interconnectivity between them (Cowton *et al.*, 2013; Tedstone *et al.*, 2015). This means that the seasonal response of each glacier to surface meltwater varies between individual glaciers and between glaciated regions (e.g. Sole *et al.*, 2013; Andrews *et al.*, 2014; Tedstone *et al.*, 2015). Equally important, however, is the observed increase in the number of glaciers worldwide which are responding rapidly to sub-aqueously driven dynamic changes (e.g. Hart *et al.*, 2011; Carrivick and Tweed, 2013; Sakakibara *et al.*, 2013; King *et al.*, 2018).

Calving fluxes, and the behaviour of calving glaciers in general, are strongly controlled by ice velocity (Meier and Post, 1987; Howat *et al.*, 2005; Benn *et al.*, 2007b; Pritchard *et al.*, 2009; Sugiyama *et al.*, 2011; Sakakibara *et al.*, 2013). This is because the majority of calving events are a consequence of crevasse propagation in response to longitudinal stress caused by fast ice flow (Meier and Post, 1987; Naruse and Skvarca, 2000; Van der Veen, 2002; Benn *et al.*, 2007b). As a glacier retreats into deeper water (e.g. down a reverse slope), the water depth and therefore the calving flux increase as a result (Schomacker, 2010). This is because glaciers flow faster when entering deeper water, due to the inverse relationship between effective pressure and basal drag, leading to rapid ice flow, thinning and retreat (Howat *et al.*, 2007; Benn *et al.*, 2007a), and such a relationship has been observed for a number of glaciers worldwide (e.g. Brown *et al.*, 1982; Pelto and Warren, 1991; Naruse and Skvarca, 2000; Warren and Kirkbride, 2003; Nick *et al.*, 2007).

Many of Iceland's glaciers have been retreating rapidly since ~1990 in response to increasing mean air temperatures, with many more showing a particularly heightened rate of retreat over the last decade (Sigurðsson *et al.*, 2007; Bradwell *et al.*, 2013). Such a response can be attributed to a mean annual temperature increase of 1°C since 2000, which is three to four times higher than the Northern Hemisphere average over the same period (Jones *et al.*, 2012), as well as a shift in atmospheric and oceanic circulation patterns around Iceland (Björnsson *et al.*, 2013; Foresta *et al.*, 2016). This has resulted in ~9.5±1.5 Gt a^{-1} of mass loss between the mid-1990s and 2010, and a loss of 5.8±0.7 Gt a^{-1} between 2010–11 and 2014–15, equating to a s.l.r. contribution of ~0.03 and 0.016 mm a^{-1}, respectively (Björnsson *et al.*, 2013; Foresta *et al.*, 2016).

This retreat has been accompanied by a sharp increase in the formation and growth of proglacial lakes at the termini of many of the southerly flowing outlet glaciers of the country's main ice caps (Hannesdóttir *et al.*, 2015; Dell *et al.*, 2019). The effect these lakes are having on these glaciers is above and beyond that of climate alone (Carrivick and Tweed, 2013; Staines *et al.*, 2015), because their development causes accelerated terminus retreat by influencing ice dynamics and velocity through calving (Haeberli *et al.*, 2016; Nie *et al.*, 2017; King *et al.*, 2018). Furthermore, the size and number of such lakes is projected to increase in the future due to continued climate warming and glacier retreat, with the resulting effect on glacier dynamics in the region likely to be significant (Björnsson *et al.*, 2001; Flowers *et al.*, 2005; Schomacker, 2010).

One glacier which has seen such proglacial lake formation and development at its margin is Breiðamerkurjökull, a large soft-bedded temperate glacier in south-east Iceland. During its Little Ice Age (LIA) advance, the glacier excavated a 200–300 m-deep proglacial trough under one of its larger, more dynamic ice lobes (Björnsson, 1996; Björnsson *et al.*, 2001), leading to a marked overdeepening under the glacier. Since this maximum, however, the glacier has retreated rapidly (Hannesdóttir *et al.*, 2015; Guðmundsson *et al.*, 2017), but as a result of this overdeepening this dynamic lobe of the glacier is now retreating down a reverse slope below sea level (Björnsson, 1996; Guðmundsson *et al.*, 2017).

Although there have been several studies undertaken on Breiðamerkurjökull in recent years (e.g. Schomacker, 2010; Voytenko *et al.*, 2015; Guðmundsson and Björnsson, 2016; Storrar *et al.*, 2017), these studies have tended to focus on small-scale velocity changes occurring over short time scales (e.g. Voytenko *et al.*, 2015), or on one aspect of glacial dynamic change such as the influence of glacier topography on ice dynamics (e.g. Storrar *et al.*, 2017).

Therefore, the aim of this study is to investigate recent velocity changes at Breiðamerkurjökull, south Iceland using satellite remote sensing to understand how the glacier is responding to recent change and evaluate the different key glaciological and morphological forcing factors. We quantify decadal changes in glacier velocity since 1991 in relation to frontal retreat, lake area change, bedrock topography and ice surface elevation change. In doing so, we have examined glacier velocity at a spatial and temporal resolution not yet attempted on Breiðamerkurjökull, enabling us to fully quantify the long-term, glacier-wide changes in dynamics that have occurred over recent decades. The conclusions from this site may be used to predict the response of other soft-bedded glaciers with subglacial reverse slopes and aquatic margins (e.g. in Iceland and Alaska) to future warming.

Data and Methods

Study area

Breiðamerkurjökull (64°9′ N, 16°24′ W) is a large, south, south-easterly flowing outlet glacier of the Vatnajökull Ice Cap, Iceland (Figure 1).

The glacier had a combined area of ┼906 km^2 in 2010, with an elevation range from ~10 to 1700 m a.s.l. (Guðmundsson *et al.*, 2017). The glacier is composed of three main lobes, or 'arms' (after Guðmundsson *et al.*, 2017), separated by two large medial moraines. The larger, eastern arm (Norðlingalægðarjökull) drains the large ice dome of Breiðabunga deep within the ice cap (Evans and Twigg, 2002). The central arm (Esjufjallajökull) flows out from the two large nunataks Máfabyggðir (1440 m a.s.l.) and Esjufjöll (1770 m a.s.l.), with the latter also giving the name to the large medial moraine (Esjufjallarönd) that separates the eastern and central arms (Guðmundsson and Björnsson, 2016). The western lobe (Máfabyggðajökull) collects ice from several glaciers on the eastern flanks of Öræfajökull before draining south of Máfabyggðir, divided from the central arm by the medial moraine Mávabyggðarönd (Guðmundsson and Björnsson, 2016; Guðmundsson *et al.*, 2017). The most western lobe is composed of two arms which we have defined as western A and B (Figure 1). Two lakes of differing sizes are also present at the glacier terminus – the large ~24 km^2, 300 m-deep Jökulsárlón (Voytenko *et al.*, 2015) adjacent to the eastern arm, and the smaller 5.8 km^2 Breiðárlón adjacent to western A. Most of glacier bed sits at, or just above, sea level, however

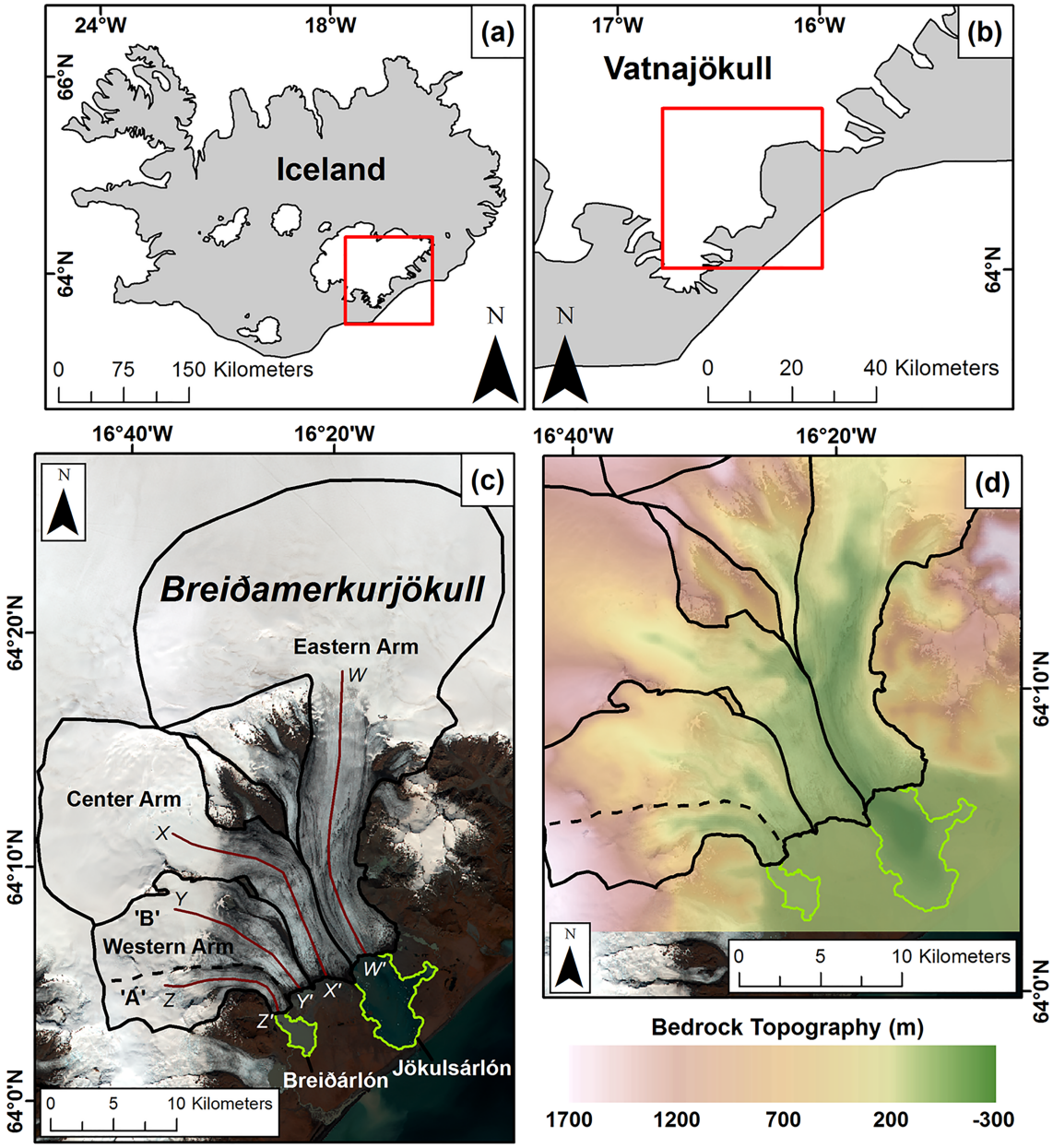

FIGURE 1. (a) Location of Breiðamerkurjökull within Iceland, and (b) within the Vatnajökull Ice Cap. (c) Area of Breiðamerkurjökull, showing each of the four main arms (black outlines), the centrelines of each arm (deep red), the start and end point of each centreline (e.g. W to W′), and the location and area (as of 2019) of Jökulsárlón and Breiðárlón (light green). Glacier outlines obtained from the GLIMS database. Centrelines derived manually using the geometry of the outlines. Nunatak outlines taken from Guðmundsson *et al.* (2017). (d) Bedrock topography of Breiðamerkurjökull, which extends down to −300m below sea level at its deepest (darkest green). Interpolated from contours provided in Björnsson (1996). Lake areas and glacier outlines as before. Background image is a Sentinel-2 acquisition (5, 3, 2 RGB) from 06/07/2019. [Colour figure can be viewed at wileyonlinelibrary.com]

a small, shallow trough runs back from the margin of western A, while a large, deep trough is found under the eastern arm, which extends back ~20km from Jökulsárlón into the glacier interior (Björnsson, 1996). This region has also seen a 1.5°C rise in the mean annual air temperature between 1980 and 2017, based on data collected by the Icelandic Met Office from their station at Fagurhólmsmýri (63°52′ N, 16°38′ W), located 5km from Breiðamerkurjökull at an elevation of 16m a.s.l.

Optical and SAR imagery

A variety of remotely sensed optical and SAR imagery was analysed in this study, including ERS-1/2 (http://esar-ds.eo.esa.int/socat/SAR_IMP_1P), TerraSAR-X (https://geoservice.dlr.de/egp/), Sentinel-1 and -2 (https://scihub.copernicus.eu/dhus/#/home), Landsat 7 ETM+ and 8 OLI/TIRS (https://earthexplorer.usgs.gov/) and 15 aerial photographs attained by the National Land Survey of Iceland, dating from 1982 to 1998 (http://www.lmi.is/en/aerial-photos/). In total, our datasets span the years 1982–2018. Table 1 summarizes the data used in this study.

Detailed characteristics of the different SAR data utilized in this study are illustrated in Table 2. For these analyses, data were downloaded from their respective archives in image precision (IMP) mode for ERS-1/2, interferometric wide-swath (IW) mode for Sentinel-1 and strip-map (SM) mode for TerraSAR-X. Where possible, data acquired in September were downloaded to allow direct comparisons to be made between years, however, this was not always possible due to the availability of data and so in these instances the nearest possible dates to September were selected. Acquisition dates for each

Table 1. List of imagery sources, imagery type, years acquired and their use in the current study

Imagery source	Image/sensor type	Years acquired	Utilization
LMS Aerial Photos	Vertical black and white aerial photo	1982, 1988, 1989, 1991, 1992, 1994, 1998	Lake area and frontal position change
Landsat 7 ETM+	Optical	2002, 2006, 2010	Lake area and frontal position change
Landsat 8 OLI/TIRS	Optical	2014	Lake area and frontal position change
Sentinel-2	Optical	2018	Lake area and frontal position change
ERS-1/2	SAR	1991, 1996, 2001, 2005	Velocity analyses
TerraSAR-X	SAR	2008, 2012, 2013, 2015	Velocity analyses
Sentinel-1	SAR	2018	Velocity analyses

Table 2. Comparison between the different SAR imagery utilized in the velocity analysis in this study

SAR satellite type	Sensor frequency (GHz)	Sensing interval (day)	Imaging mode	Swath (km)	Resolution (m)
ERS-1/2	5.3	35 (standard)	IMP	100	30
TerraSAR-X	9.6	11	SM	30	2
Sentinel-1	5.4	12	IW	250	10

SAR image used in the velocity analyses, as well as the time between each pair for each year, are given in Table 3. Overall, the dataset spans 1991–2018.

Glacier-wide velocities

All data were analysed and processed using the Sentinel Application Platform (SNAP) (ESA, 2016), the freely available ESA-developed software toolbox for analysing ESA products (//step.esa.int/main/download/). All sets of data were processed using the well-established offset-tracking methodology (Lu and Veci, 2016). Precise orbital vectors were first applied to each individual SAR acquisition to provide accurate satellite position and velocity information for each product (Serco Italia SPA, 2018), before sub-setting each image to the area of Breiðamerkurjökull to streamline processing. Digital elevation model (DEM)-assisted co-registration was then undertaken on pairs of images for each period using the LiDAR DEM of Iceland (Landmælingar Íslands, 2016). The DEM has a resolution of 10×10 m and was updated in 2016 to include elevation data for all glaciers in Iceland (Landmælingar Íslands, 2016). The LiDAR DEM was preferred to ArcticDEM, as the former was deemed to be of better quality and, therefore, would be capable of ensuring more accurate image co-registration (Heid and Kääb, 2012). This process was performed on each image pair before offset tracking was undertaken on the resulting stacked images. All images for each sensor type were processed using the exact same parameters to ensure spatial coverage did not vary between images, allowing direct comparisons to be made between sensor types (Table 4).

Offset tracking estimates the movement of glacier surfaces between master and slave images in both the slant range and azimuth direction through cross-correlation on selected ground control points (GCPs) (Dehecq *et al.*, 2015; Nagler *et al.*, 2015; Fahnestock *et al.*, 2016; Serco Italia SPA, 2018). The glacier velocity is computed based on the offsets estimated by the cross-correlation algorithm before the final velocity map is generated through interpolation of the velocities computed on the GCP grid (Lu and Veci, 2016). Displacement vectors larger than 5 m day^{-1} or with a correlation coefficient less than 0.1 were removed. The displacement vectors were then averaged over a 20×20 pixel grid to create the velocity raster. The holes left by the anomalous values were then filled by replacing each missing point with a new offset computed by locally weighted average (Serco Italia SPA, 2018). The final velocity maps were subsequently terrain-corrected using the LiDAR DEM of Iceland to convert between slant-range and ground-range coordinates. To allow for a more robust comparison of the velocity data between years to be made, we present mean velocity measurements taken at 1 km intervals along the glacier centrelines (shown in Figure 1). Furthermore, although we used images from approximately the same period each year, we wanted to investigate the effect of seasonality on our data, and test whether the velocity change we observed for the eastern arm reflected actual change, or simply seasonal variation. To do so, we utilized several TerraSAR-X images covering 24 July–11 November 2008 and processed them following the same method as was used for the velocity analyses.

Lake area and terminus position changes

To assess lake area change for both Jökulsárlón and Breiðárlón, the individual lake areas were manually digitized in ArcGIS 10.7 for 11 time steps between 1982 and 2018 using a

Table 3. Acquisition date of each of the image pairs used in this study to calculate glacier velocity. Time between each pair is also shown

Satellite type	Image date for $t = 1$	Image date for $t = 2$	Time between pairs (days)
	12 August 1991	23 October 1991	72
	29 August 1996	3 October 1996	35
	6 August 2001	10 September 2001	35
ERS-1/2	28 July 2005	1 September 2005	44
	6 September 2008	28 September 2008	22
	26 July 2012	17 August 2012	22
	26 August 2013	17 September 2013	22
TerraSAR-X	26 May 2015	17 June 2015	22
Sentinel-1	24 August 2018	5 September 2018	12

Table 4. Processing parameters utilized in SNAP to obtain the velocity outputs for each of the three SAR sensor types

Satellite type	Grid azimuth spacing (pixels)	Grid range spacing (pixels)	Registration window width/height	Max. velocity ($m day^{-1}$)	Cross-correlation threshold
ERS-1/2	20	20	256 × 256	5	0.1
Sentinel-1	20	20	256 × 256	5	0.1
TerraSAR-X	20	20	256 × 256	5	0.1

combination of black and white orthorectified aerial photographs and Landsat and Sentinel-2 imagery. Information about each of the aerial photos used in this study is given in Table 5. Manual digitization was preferred to automated normalized difference water index (NDWI) image classification because turbid water can often have varying NDWI values, resulting in lakes being classified as glacier ice and thus hindering our ability to accurately delineate lake area through time (Racoviteanu *et al.*, 2009; Gjermundsen *et al.*, 2011).

The individual photos were first orthorectified and then georeferenced to a base image with known coordinates. This was undertaken in ArcGIS by marking on stable points within each individual aerial photo and then finding the same points in a Landsat OLI acquisition from 2018. A Landsat OLI acquisition was utilized as the base image due to its low geolocation errors (Dell *et al.*, 2019). All aerial photos were georeferenced with a root mean square error of less than 0.5 pixels. Lake areas were then digitized at a scale of 1:6000 for the aerial photographs and 1:10000 for the Landsat and Sentinel-2 imagery. These scales allowed the accurate mapping of the lake areas and prevented pixelated images hindering reliable interpretation (Lovell, 2016; Dell *et al.*, 2019). Channels that exited the lake (such as the one flowing from Breiðárlón into the neighbouring Fjallsárlón) were ignored during the digitization at the point where the channel began to form.

Terminus position changes for each of the main arms of Breiðamerkurjökull were assessed using the same imagery, time steps and digitizing scale used to quantify lake area change. At each time step, the position of the terminus for each of the main arms was manually digitized. To calculate the positional change through time for each arm, the rectilinear box method was implemented (Moon and Joughin, 2008; Howat and Eddy, 2011), which quantifies the change in area between different terminus positions using a fixed-width rectilinear box drawn over the glacier trunk. This was then converted to a 1-D figure by dividing the change in area by the change in terminus width (Howat and Eddy, 2011; Lea *et al.*, 2014). This method was chosen for this study due to its ability to account for asymmetrical changes at the calving front (Lea *et al.*, 2014; Larsen *et al.*, 2016; Dell *et al.*, 2019), while other methods, such as automatic ice classification of Landsat images, can be influenced by turbid water, and it cannot be used for aerial photos, which would hinder its use in this analysis (Gjermundsen *et al.*, 2011). When assessing the change occurring at the calving front of the eastern arm and western A, the width of the box used encompassed the maximum delineated width of the lake-terminating portion of the front (1992 for Jökulsárlón, 1989 for Breiðárlón) rather than the whole terminus of both arms. This ensured that the captured rate of positional change actively related to what was occurring at the calving front.

Ice surface elevation change

Changes in the ice surface elevation of Breiðamerkurjökull were examined using the freely available ArcticDEM dataset distributed by the Polar Geospatial Centre (Porter *et al.*, 2018) (https://www.pgc.umn.edu/data/arcticdem). This dataset provides digital surface models (DSMs) at a spatial resolution of 2 m for areas north of 60° from 2011 in most regions (Morin *et al.*, 2016). Data are typically downloaded as 17×110 km strips (Barr *et al.*, 2018). In the case of Breiðamerkurjökull, the data coverage is particularly good, with several DSMs available covering varying extents of the glacier for different years. We chose two DSMs for this analysis, one from 05/10/2012 and the other from 20/10/2017 as both DSMs covered the entire glacier area, while also affording us the opportunity to investigate surface elevation change associated with glacier recession. The DSMs were linearly co-registered following the method of Nuth and Kääb (2011).

Uncertainty analyses

Velocity uncertainty

To determine the uncertainty of our velocity measurements, we measured displacements over terrain that we regarded as stable (Robson *et al.*, 2018). We carried out this analysis over two different areas (Figure 2) before calculating the combined stochastic error of both. The first was restricted to an area ~1 km away from the land-terminating portion of Breiðamerkurjökull, on a portion of presumably stable ground situated between both proglacial lakes that was free from shadow and had little or no surface slope. The second was placed on sloping, but stable, ground to the right of Breiðamerkurjökull to assess the accuracy

Table 5. Key information regarding each of the aerial photos downloaded and utilized in this study for the lake area and terminus position change analysis

Date acquired	Resolution (m)	Altitude (m)	Focal lens length (mm)	Area of interest
20/08/1982	<1	6100	151-78	Jökulsárlón and Breiðárlón
22/08/1988	<1	5486	151-76	Jökulsárlón and Breiðárlón
31/07/1989	<1	5486	151-76	Jökulsárlón Breiðárlón
21/08/1991	<1	6066	151-78	Breiðárlón
04/08/1992	<1	5486	151-78	Jökulsárlón
09/08/1994	<1	5486	152-82	Jökulsárlón Breiðárlón
22/08/1998	<1	4600	153-15	Jökulsárlón Breiðárlón

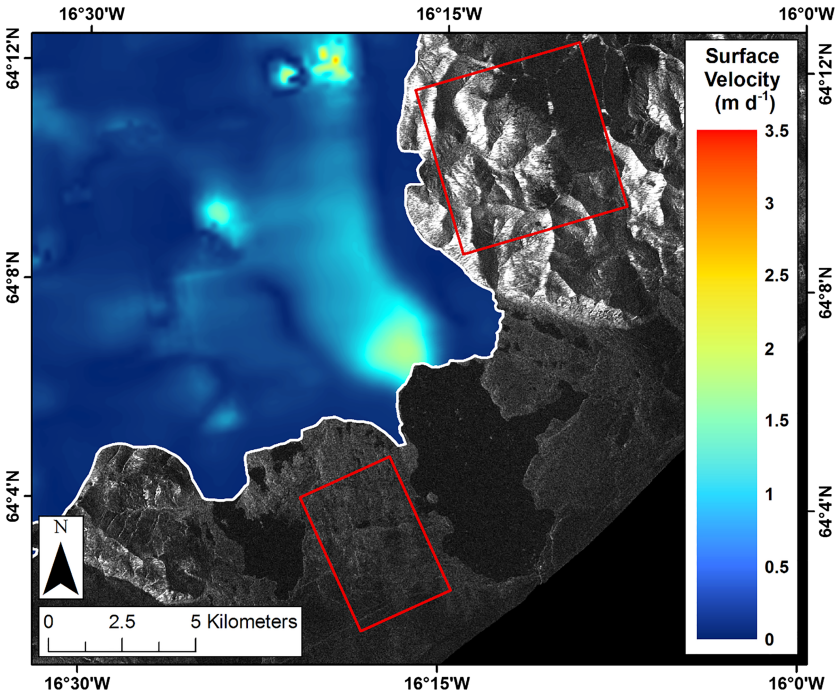

FIGURE 2. Areas used as 'stable ground' (red boxes) to calculate the stochastic error in our velocity data. Velocity output and glacier outline for 2018 (white line) shown for reference. Background is a Sentinel-1 terrain-corrected SAR image from 05/09/2018. [Colour figure can be viewed at wileyonlinelibrary.com]

of the co-registration process. Generally, we find that mean stochastic uncertainties for each satellite sensor are somewhat similar. Calculated values are greatest for the ERS-1/2 data, with a mean error of ±0.19 m, while for TerraSAR and Sentinel-1 the error is ±0.14 and ±0.11 m, respectively, indicating that the levels of uncertainty we estimate are not greater than the change in velocity over the duration of our study.

Digitization uncertainty

To quantify the uncertainty when digitizing the lake areas and glacier frontal positions, the areas of Jökulsárlón and Breiðárlón in 1982, 2014 and 2018 were repeatedly digitized 10 times at the same scale as used in the initial analyses. Key statistical values, including the coefficient of variation (CV) and standard uncertainty, or standard error (SE) were then calculated to allow comparisons to be made between the three different sets of aerial imagery (Table 6). Importantly, the calculated uncertainties for all image types are not greater than the change observed in our analyses.

Surface elevation change uncertainty

The uncertainty of the elevation changes was calculated by combining the standard error with the mean vertical bias over the terrain that was assumed to be stable (i.e. on non-glacier terrain) (Nuth *et al.*, 2012; Robson *et al.*, 2018). The SE takes into account standard deviation over stable terrain (SD_{STABLE}) and the number of independent pixels included in the DEM differencing (n):

$$SE = \frac{SD_{STABLE}}{\sqrt{n}} \quad (1)$$

n is determined by the original number of pixels in the DEM differencing analysis (N_{tot}), the pixel size (PS) and spatial autocorrelation (d), which we assumed to be 600 m:

$$n = \frac{N_{tot}.PS}{2d} \quad (2)$$

DEM differencing uncertainty was then calculated by combining the standard error with the mean vertical bias on stable ground, following the method of Robson *et al.* (2018). This gave an elevation error on stable ground of ±0.45 m over the period 2012–2017, equating to 0.09 m year^{-1}, indicating that our elevation assessment is highly accurate.

Table 6. Statistical values calculated to quantify digitization error for the analyses undertaken in this study, including mean area, CV and standard uncertainty

Imagery type	Proglacial lake	Original measured area (km^2)	Mean repeat area (km^2)	Standard deviation (km^2)	CV (%)	Standard uncertainty (±km^2)
Aerial photo (<1 m)	Jökulsárlón	7.58	8.039	0.009	0.11	0.003
	Breiðárlón	5.39	5.407	0.003	0.06	0.001
Landsat 8 (15 m)	Jökulsárlón	24.39	24.978	0.031	0.12	0.010
	Breiðárlón	5.67	5.670	0.035	0.62	0.011
Sentinel-2 (10 m)	Jökulsárlón	27.2	26.801	0.018	0.07	0.006
	Breiðárlón	5.85	5.802	0.012	0.21	0.004

Results

Glacier-wide velocities

Surface velocity 1991–2018

We observe spatially variable velocity change for Breiðamerkurjökull over the period 1991–2018 (Figure 3). The calculated velocity observations (Figure 3) show that the highest velocity values for the study period are consistently found for the eastern trunk, particularly from 2008 onwards. Maximum values increased from ~0.65 ±0.15 m day^{-1} in 2001 to ~3.50 ±0.25 m day^{-1} by 2015, before dropping to ~1.72 ±0.11 m day^{-1} in 2018. Such a trend is also observed in the full velocity dataset (see Figure S1 in the online Supporting Information), despite maximum velocities first decreasing slightly between 1991 and 1996, from ~1.00 ± 0.36 to ~0.55 ±0.11 m day^{-1}, before then increasing again until 2015.

The mean velocities for the years 2001–2018, calculated using the glacier flowlines, indicate that the greatest change in mean velocities over the period is observed for the eastern arm (Figure 4; full dataset shown in Figures S2–S5 of the online Supporting Information). Between 2001 and 2005, mean velocities over the whole trunk of the eastern arm remained stable, apart from a slight peak in velocities near the calving front of 0.58 ±0.15 and 0.44 ±0.12 m day^{-1} observed for 2001 and 2005, respectively. From 2008 onwards, however, the mean velocity remained elevated and increased year on year, particularly in the near-terminus region. Peak near-terminus velocities in 2008 were 1.58 ±0.09 m day^{-1}, jumping to 1.63 ±0.11 m day^{-1} in 2012, increasing slightly to 1.64 ±0.15 m day^{-1} in 2015, before peaking at 1.68 ±0.11 m day^{-1} in 2018. No such dynamic changes were observed at the other three arms over the same period.

Mean velocities for the central arm remained stable between 2001 and 2018, with very little yearly variation observed. Indeed, apart from a peak in near-terminus velocities of 0.49 ±0.15 m day^{-1} in 2001, the observed general trend from 2001 onwards is one of decreasing velocities down-glacier right up to the margin. Indeed, a similar scenario is also found for both

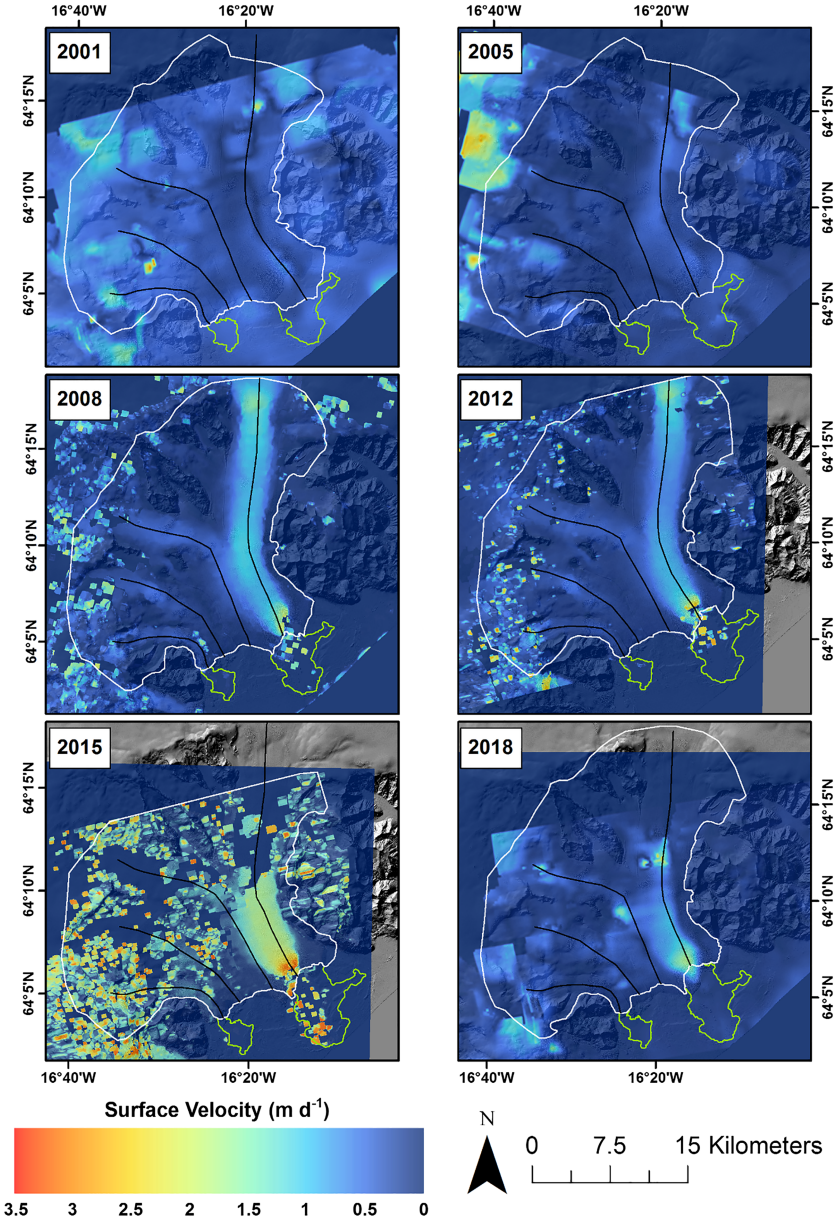

FIGURE 3. SNAP-obtained velocity outputs for selected years covering our study period. We choose to display the data from 2001 onwards as the most significant changes in velocity are found to be occurring after this date, and are therefore of most interest in this study. All outputs shown at 20% transparency overlaid on a hillshade of the LiDAR DEM of Iceland from 2016. Longitudinal flowlines are also shown. Glacier outlines (white) and lake areas (light green) are from each respective year. [Colour figure can be viewed at wileyonlinelibrary.com]

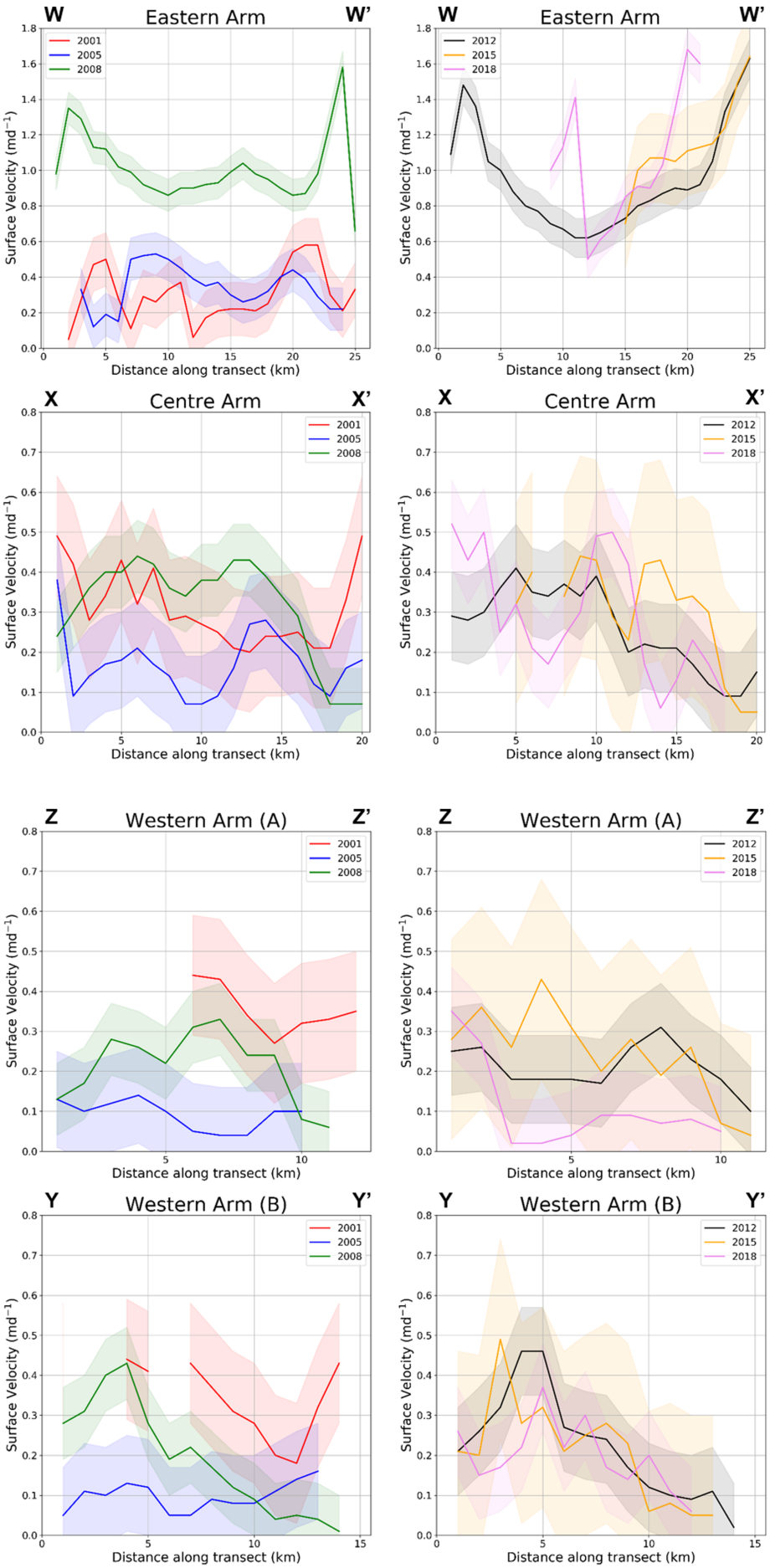

FIGURE 4. Velocity profiles for all four arms of Breiðamerkurjökull for the period 2001–2018, calculated by taking the mean velocity at 1 km segments along the entire length of the glacier flowlines show in Figure 1. Associated uncertainty margins for each year are also shown. [Colour figure can be viewed at wileyonlinelibrary.com]

western A and western B, with the former having the lowest overall velocities for any arm of Breiðamerkurjökull, particularly from 2008 onwards.

Seasonality analysis

The results of our seasonality analysis (Figure 5) indicate that, despite there being some variation (which we infer to be seasonal variation), overall the velocity signal is stable and does not show any large variations from the mean, which is particularly true for the terminus region (>22 km along transect). Alongside this we have also plotted the velocity series covering our study period to investigate how these differ from the data for 2008.

This clearly shows that in 2012 (the next closest data series to 2008), the velocity values are not significantly different to 2008, apart from in the near-terminus region where velocities are greater. Conversely, the data from 1991 to 2005 sit well outside the data margins from 2008, indicating that this data is significantly different from the 2008 data. Furthermore, it also reinforces the inference that the most significant changes are occurring in the near-terminus region (i.e. with increasing velocities from 2008). This indicates that the velocity change observed in 2008, and in the other years of our analysis, likely reflects actual long-term change, and not natural seasonal variability.

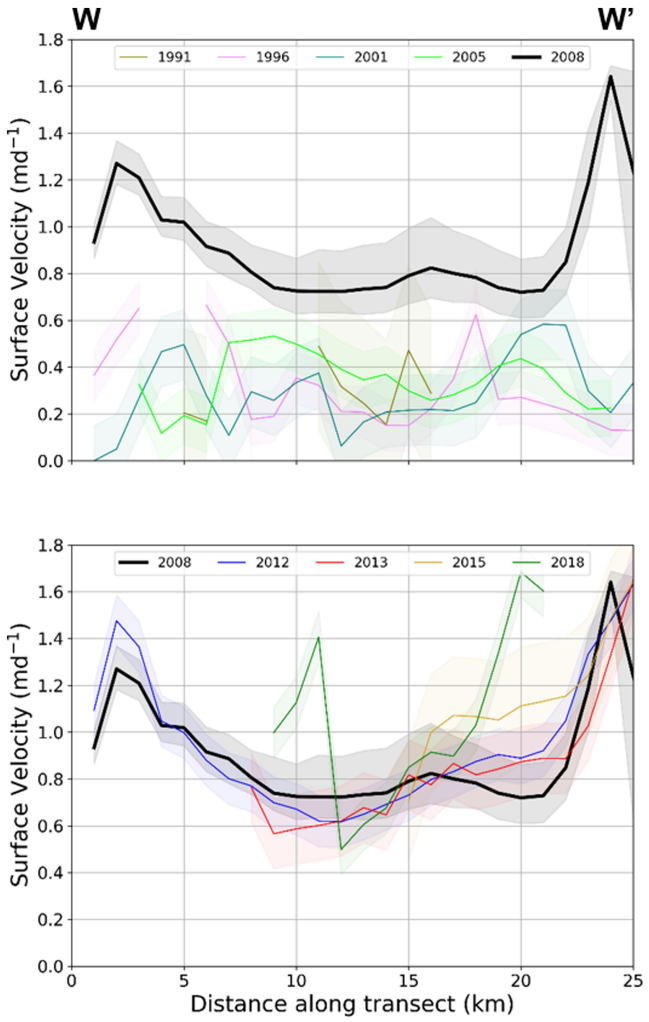

FIGURE 5. Combined mean velocities from 2008 for the eastern arm of Breiðamerkurjökull to assess the influence of seasonality on our velocity results (thick black line). The maximum and minimum velocity found at each distance for each of the raster datasets from 2008 are shown as the grey shaded margins. Velocity profiles for all years (along with their relative uncertainty margins) are also plotted for comparison. [Colour figure can be viewed at wileyonlinelibrary.com]

Lake area and frontal position change

The areas of both Jökulsárlón and Breiðárlón have increased over the research period, although at vastly different rates (Figure 6). The area of Jökulsárlón increased from 7.58 to 27.20 km^2 (Figure 7), an overall increase of nearly 270% between 1982 and 2018. This equates to an overall lake growth since 1982 of ~0.55 km^2 year^{-1}. In comparison, the area of Breiðárlón increased only very slightly, from 5.39 km^2 in 1982 to 5.84 km^2 in 2018 (Figure 7), equating to an increase of 8.36% (the uncertainty values for this analysis were <1%, see Table 6).

Over the study period, the land-terminating arms of the glacier seemed to be retreating at a steady rate between 1982 and 2018, with these arms all displaying similar rates of retreat from 1982 onwards (Figure 8). However, while the retreat of the lake-terminating portion of the eastern arm between 1982 and 1992 seemed to be occurring at a similar rate to that of the rest of Breiðamerkurjökull, after this point rapid changes started to occur. Overall, this portion of the eastern arm has retreated by ~3.50 km, or 92.69 m year^{-1} (Figure 7). Particularly rapid retreat occurred between 2002 and 2014, at a rate of 470.25 m year^{-1}. Similar retreat rates are not evident for any other arms of Breiðamerkurjökull, land-terminating or otherwise. Interestingly, for western A, which flows into Breiðárlón, we observe a retreat of ~1.11 km, equating to a rate of 31.09 m year^{-1} (Figure 7), the smallest overall change for the study period.

Ice surface elevation change

Between 2012 and 2017, significant thinning has occurred at the margin of the eastern arm where it terminates into Jökulsárlón, with 100–130 ±0.45 m of negative surface elevation change observed (Figure 9). Furthermore, this thinning has occurred ~2–3 km back from the margin along the entire width of the calving front, with 60–80 ±0.45 m of negative change observed, which is greater than the change observed at the other three lobes over the same period. Comparatively small elevation changes are observed for western A and B, with ~20 ±0.45 m of negative change observed for the former in particular, while the margin of the central arm thinned by ~50 ± 0.45 m. Meanwhile, slightly positive changes of 0–10 ±0.45 m are observed over the higher reaches of the glacier.

Discussion

Velocity change 1991–2018

We have presented the first multi-year and highly detailed velocity analyses of Breiðamerkurjökull covering almost three decades using high-resolution SAR offset-tracking techniques. Our data illustrate a clear increase in surface velocities for the eastern arm since 1991, with heightened velocity increases occurring from ~2008 up to 2015, where values of up to 3.50 ±0.25 m day^{-1} were recorded in the near-terminus region. This is in stark comparison to the other three arms of Breiðamerkurjökull, where we do not detect any change beyond the uncertainty of our methods. Such a contrast is likely due to the highly dynamic nature of the eastern arm and its close relationship with the growth of the Jökulsárlón lagoon, which has caused an increase in ice acceleration and retreat (Benn *et al.*, 2007a; Schomacker, 2010). This relationship will

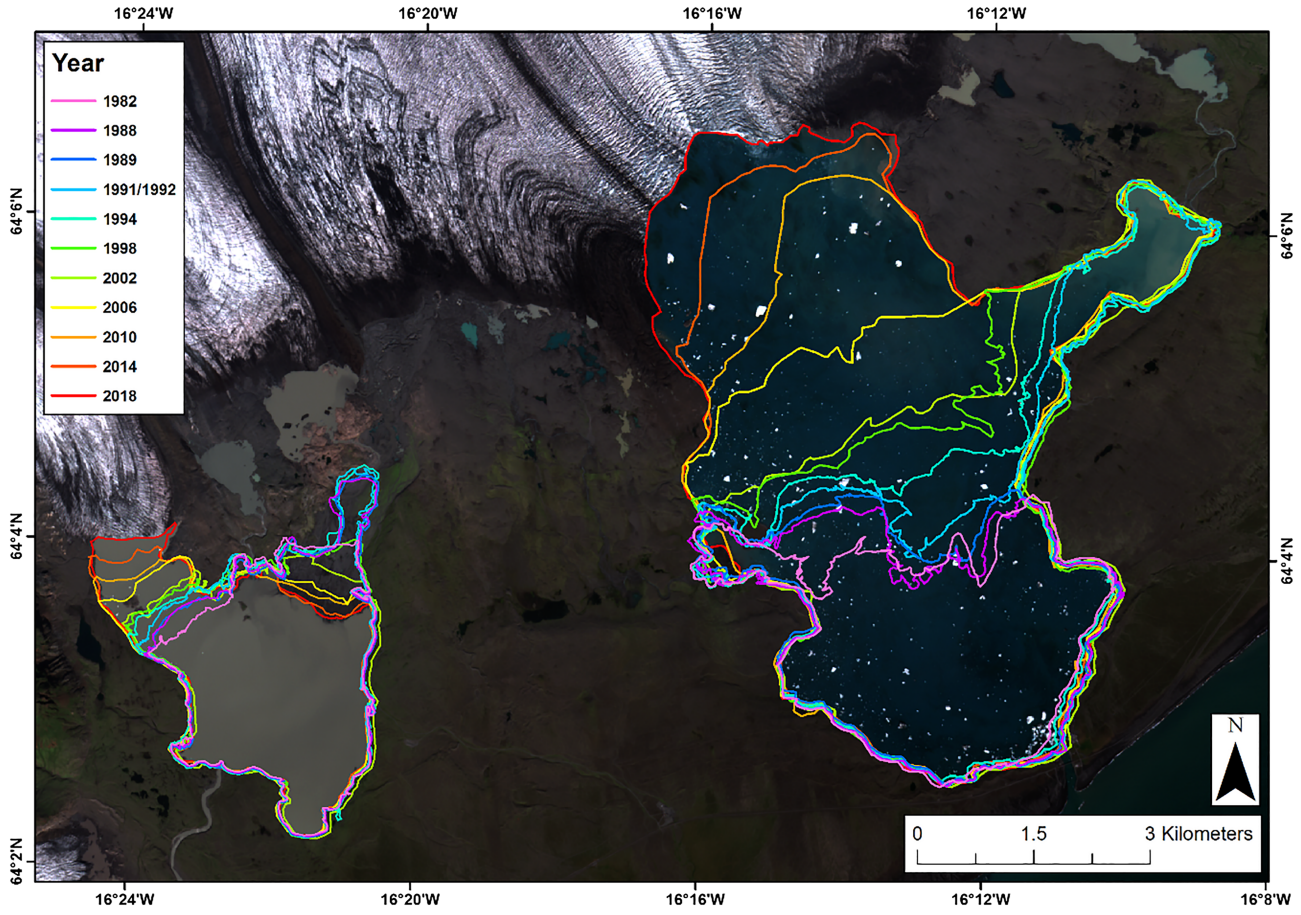

FIGURE 6. Change in lake area since 1982 for Jökulsárlón and Breiðárlón from digitization of successive imagery. Background image is a Sentinel-2 true colour acquisition from 22/08/2018. [Colour figure can be viewed at wileyonlinelibrary.com]

be discussed in more detail below. Our data are comparable with the few other studies that have investigated the highly dynamic nature of the eastern arm over the same period. For example, Howat *et al.* (2008), using an automated surface-feature tracking method on repeat ASTER images acquired in the summer of 2005, found that in the near-terminus region the eastern arm had an annual flow of ~550 m year^{-1}. This equates to ~1.5 m day^{-1}, putting it directly in line with the values of 1–3.5 m day^{-1} recorded in this study between 2008 and 2018. Similarly, Nagler *et al.* (2012) found surface velocities of <2 m day^{-1} for the eastern arm using TerraSAR-X data from 2010. Interestingly, Voytenko *et al.* (2015), in their analyses of the calving front between 2011 and 2013 using terrestrial radar interferometry (TRI), found daily values of up to 5 m day^{-1}, which is much faster than anything we have found in this study, particularly for our ERS and Sentinel data. However, the authors attributed such values to the high temporal resolution of the TRI, where the short averaging times for data acquisition were likely capturing short-lived dynamic phenomena that are smoothed in the longer time-averaged satellite data, even for high-resolution TerraSAR-X data (Voytenko *et al.*, 2015).

It is worth discussing why we seemingly observe a decrease in velocities for the eastern arm between 2015 and 2018 (Figure 3). This decrease may be due to glaciological or geomorphological factors that have caused glacier slowdown, or it could indicate that the change in resolution between different satellite sensors is influencing the velocity estimates during this time, rather than the decrease being representative of wholesale glacier slowdown.

The observed slowdown of some lake-terminating glaciers elsewhere over recent years has been attributed to a combination of reduced driving stress and increased resistive stresses as the terminus of these glaciers narrow, in association with surface thinning (Pimentel *et al.*, 2010; Adhikari and Marshall, 2012; King *et al.*, 2018). Increased thinning, forced by sustained periods of ice-front retreat and glacier acceleration, causes the surface slope to flatten, reducing the driving stress up-glacier and, therefore, reducing overall ice velocities (Cuffey and Paterson, 2010; King *et al.*, 2018). At Breiðamerkurjökull, an area of flat surface topography immediately behind the calving front of the eastern arm has been observed in several studies (e.g. Evans and Twigg, 2002; Guðmundsson and Björnsson, 2016; Storrar *et al.*, 2017). Here, the surface slope is only thought to be ~2°, whereas at the calving front the slope is ~14° (Voytenko *et al.*, 2015). This area of flat topography is thought to coincide with the deepest part of the subglacial trough (Evans and Twigg, 2002; Storrar *et al.*, 2017), and its area has grown in recent years as the glacier continues to thin and retreat at an increased rate (Guðmundsson and Björnsson, 2016; Storrar *et al.*, 2017). This reduction in surface slope may have caused a reduction in the driving stress since ~2015, which, therefore, might explain why we see a decrease in velocities between 2015 and 2018. However, this is beyond the scope of this paper and as such will not be addressed in any further detail.

The change in sensor resolution could also explain the observed decrease in velocities, because errors can persist when using Sentinel-1 to map slower-moving areas of ice compared to when using TerraSAR-X imagery due to the impact of ionospheric noise and temporal decorrelation (Nagler *et al.*, 2015). Equally, where sharp velocity gradients are present, such as at the terminus of Breiðamerkurjökull, the higher resolution of TerraSAR-X allows such changes in velocity to

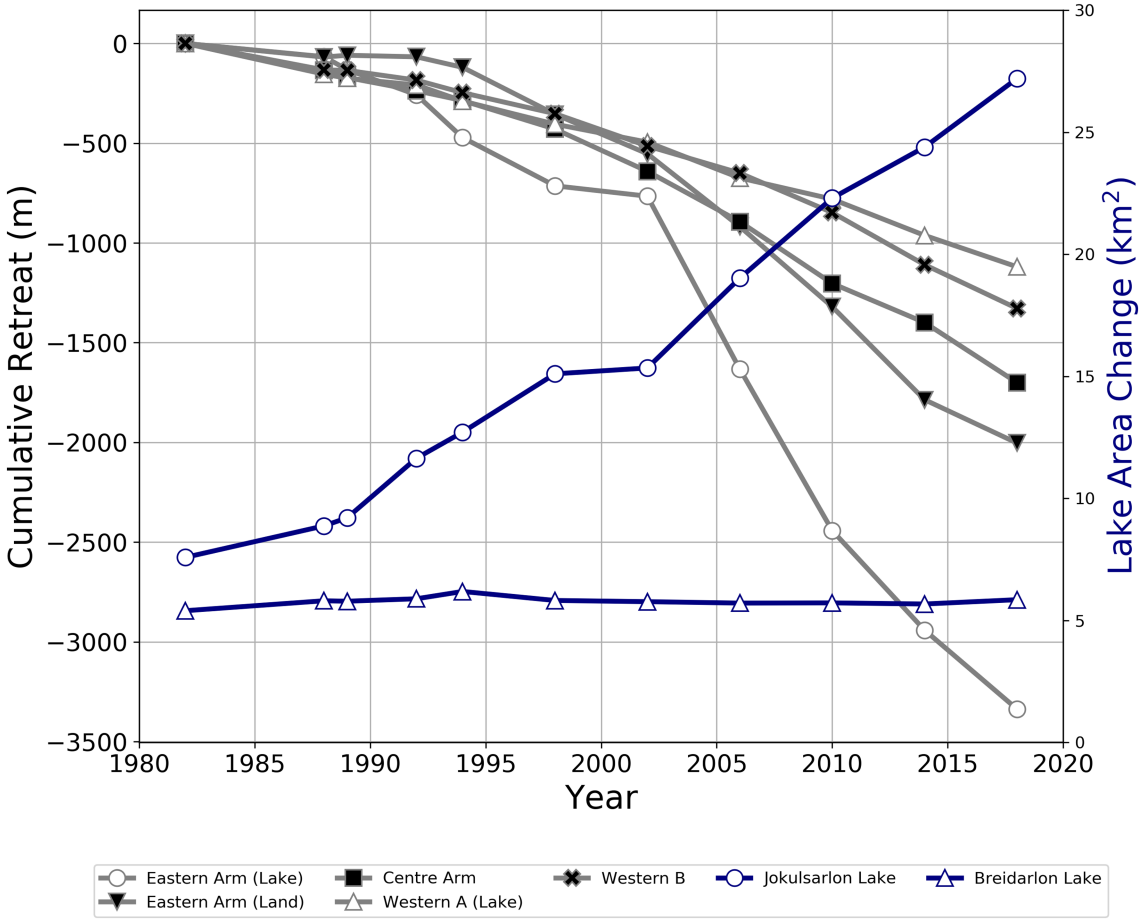

FIGURE 7. Lake area change for Jökulsárlón and Breiðárlón since 1982 versus the cumulative retreat for all terminus regions of Breiðamerkurjökull over the same period. Note that the two lake-terminating portions of the glacier have the same marker style as the lake that they terminate into. [Colour figure can be viewed at wileyonlinelibrary.com]

be tracked, whereas Sentinel-1 will tend to smooth over such gradients due to coarser image resolution (Joughin *et al.*, 2018). Similar issues can also persist when using ERS data due to its much coarser 30 m resolution, as well as the fact that ERS data can often give noisier velocity estimates due to weaker intra-pair correlation caused by surface changes over slower-moving areas (Joughin *et al.*, 2018). To test this, we resampled our TerraSAR-X outputs to 10 and 30 m resolution before comparing these to the originals. We found that the only difference was a loss of detail from the higher-resolution outputs and more smoothing in the coarser-resolution outputs. No significant differences between the outputs were observed. This suggests that although the change in pixel resolution has had an impact on our velocity estimates, the impact overall is low, further highlighting the validity of our observations. We believe, therefore, that our data strongly indicate that substantial changes in the velocity of Breiðamerkurjökull have occurred between 1991 and 2018.

Lake growth and frontal retreat 1982–2018

We have calculated lake area change and cumulative retreat for Breiðamerkurjökull for a period covering nearly four decades, indicating substantial lake growth and frontal retreat, particularly since the turn of the century. Our growth rate for Jökulsárlón of 0.55 km^2 $year^{-1}$ since 1982 shows close agreement with the values of 0.5 and 0.61 km^2 $year^{-1}$ put forward by Björnsson *et al.* (2001) and Schomacker (2010), respectively. The greater value found by the latter is due to the author investigating lake change over a 10-year period from 1999 to 2009, rather than from 1982 to 2018 as we have done in this study. However, if we average our data over a similar period (from 1998 to 2010, equating to 12 years, not 10), we find an annual growth rate of 0.6 km^2 $year^{-1}$, indicating good agreement with the findings of Schomacker (2010). Furthermore, our data are also coincident with the continued growth and development of other proglacial lakes in Iceland, particularly for the outlets of Vatnajökull, over the same period (Schomacker, 2010; Magnússon *et al.*, 2012; Dell *et al.*, 2019).

Our results also share similarities with the results of those studies which have investigated long-term proglacial lake development and growth in the Himalaya (e.g. Nie *et al.*, 2017; King *et al.*, 2018). One such study by Zhang *et al.* (2019) examined the development of 23 proglacial lakes in the Poiqu River basin, central Himalaya, from 1964 to 2017. The authors found that lake area increased at a rate of 0.23 ±0.01 km^2 between 1964 and ~2010, with the most rapid increase in area observed for the ~30 years immediately following initial lake development. From 2010 onwards, growth rates decreased significantly to 0.03 ±0.03 km^2, which the authors attributed to the fact that many lakes had reached their maximum extent by this time, becoming bounded by an abrupt steepening of valley topography, which limited further growth (Zhang *et al.*, 2019). As we have seen in this study, the area of Jökulsárlón has increased steadily since 1982, with particularly large increases in area occurring since ~2006 (Figure 7). These heightened rates of lake growth are likely to be sustained over the coming decades while the glacier continues to retreat through its 22 km-long, 300 m-deep subglacial trough, and will only start to decrease and stabilize once the glacier retreats out of the trough and the lake becomes constrained by its

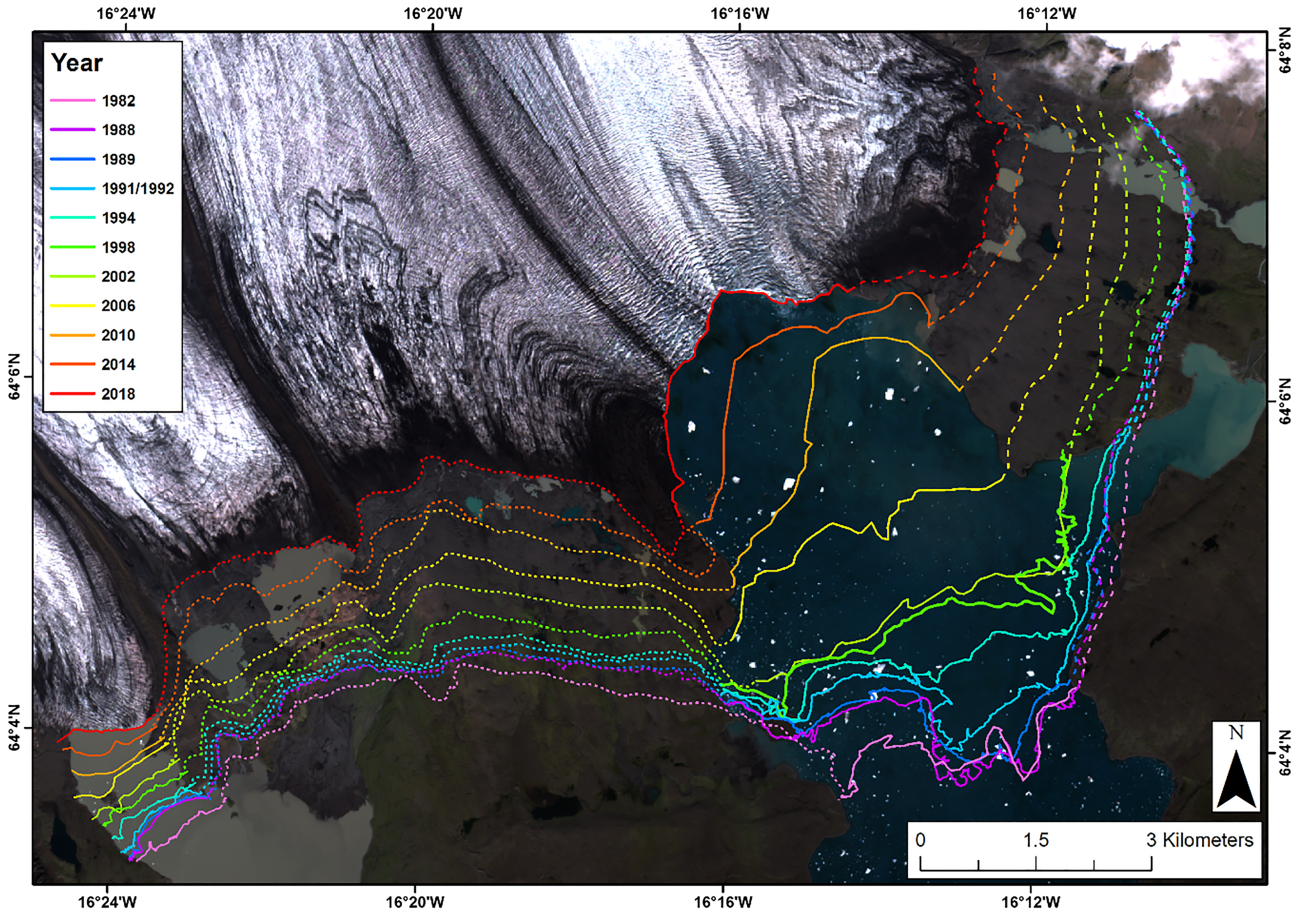

FIGURE 8. Change in the frontal position of Breiðamerkurjökull since 1982 from digitization of successive imagery. The thick and dashed lines relate to the aqueous- and land-terminating margins, respectively. Background image is a Sentinel-2 true colour acquisition from 22/08/2018. [Colour figure can be viewed at wileyonlinelibrary.com]

topography (Flowers *et al.*, 2005; Nick *et al.*, 2007). We suggest, therefore, that Jökulsárlón has recently entered a stage in its development characterized by rapid increases in area, and that these increased rates will likely continue over the decades to come.

Our retreat data also shows strong agreement with other rapidly retreating outlet glaciers in Iceland (e.g. Bradwell *et al.*, 2013; Hannesdóttir *et al.*, 2015; Einarsson, 2017), particularly those that terminate in proglacial lakes (Schomacker, 2010; Dell *et al.*, 2019). Our value of ~3.50 km of retreat since 1982 for the eastern arm is in the same order of magnitude as the 2 km measured by Einarsson (2017) for the land-terminating portion of the eastern arm for the period 1982–2014.

Interactions between lake growth, frontal retreat and ice velocity

The clear increase in velocity observed at Breiðamerkurjökull over the study period is likely to have been caused by the close relationship that exists between lake growth, ice acceleration and terminus retreat (Storrar *et al.*, 2017). The fact that the observed velocity increase is most dramatically associated with the lake growth at the margin of the eastern arm indicates the importance of Jökulsárlón in forcing the behaviour of this part of Breiðamerkurjökull. As the glacier has continued to retreat over the last few decades in response to warming air temperatures, it has receded into the large, 200–300 m-deep subglacial trough that it excavated during its LIA advance (Figure 1) (Björnsson *et al.*, 2001; Guðmundsson and Björnsson, 2016). Consequently, the area, and importantly the depth, of Jökulsárlón has increased in response as meltwater infills the overdeepened basin (Schomacker, 2010). This increase in lake depth caused the glacier to flow faster as it entered deeper water due to the inverse relationship that exists between effective pressure and basal drag (Warren and Kirkbride, 2003; Howat *et al.*, 2005; Benn *et al.*, 2007a). This would have resulted in an increase in longitudinal strain rates and fracture propagation at the terminus, leading to a corresponding increase in calving activity and, therefore, the rate of retreat (Nick *et al.*, 2007; Benn *et al.*, 2007a; King *et al.*, 2018). Further retreat down this reverse slope into the subglacial trough has caused the lake depth to increase further, causing more rapid flow acceleration, calving and retreat to occur, driving a positive feedback mechanism (Howat *et al.*, 2007). This mechanism is exacerbated by the fact that ice flow from the interior of Breiðamerkurjökull cannot balance the substantial losses occurring at the terminus, leading to further rapid acceleration, retreat and lake growth (Björnsson *et al.*, 2001; Nick *et al.*, 2007).

Moreover, it has been stated by Storrar *et al.* (2017) that this arm of Breiðamerkurjökull is currently retreating over the deepest part of the subglacial trench, and as such, water depth is also likely to be at its deepest as a result (Figure 1). This means that, all other factors considered, ice velocity is likely to have reached its maximum over the last several years in response to this significant deepening of the lake. Indeed, we found daily velocity values of up to 3.50 ±0.25 m day^{-1} at the calving front in 2015 where the trench, and therefore the water depth, is likely to be at its deepest (Björnsson *et al.*, 2001; Voytenko *et al.*, 2015). Therefore, while initial retreat at Breiðamerkurjökull was instigated by rising air temperatures

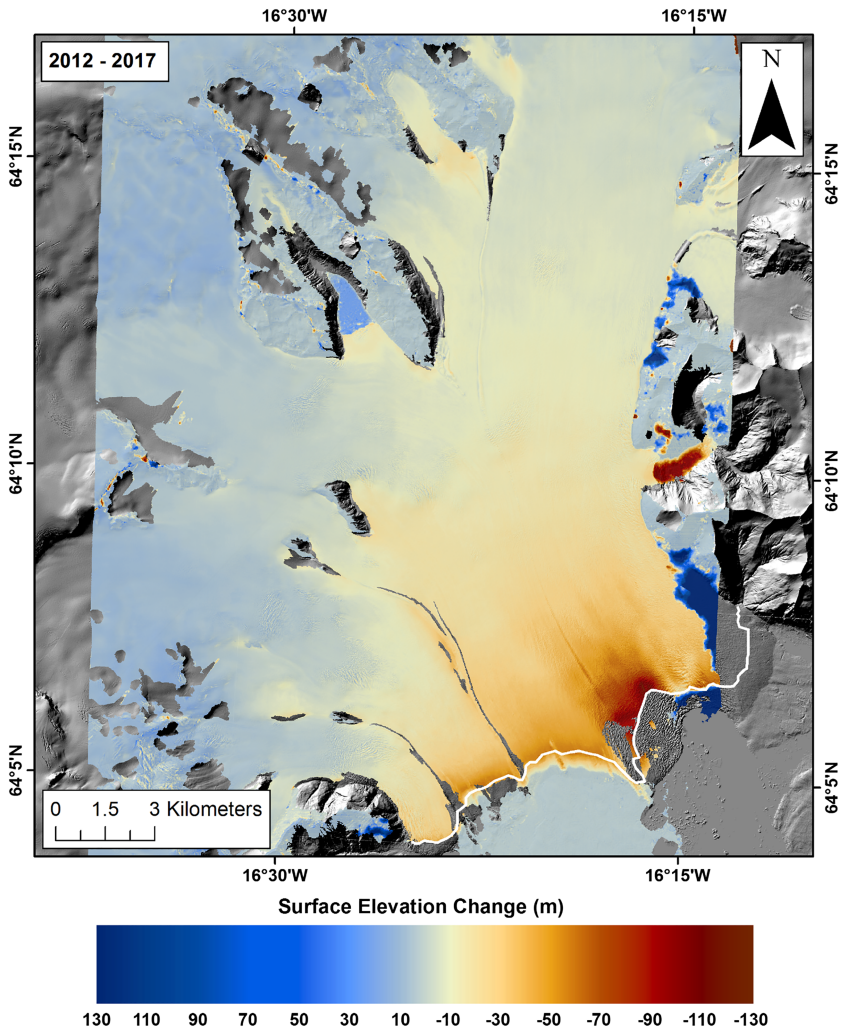

FIGURE 9. Ice surface elevation change at Breiðamerkurjökull for the period 2012–2017. White line indicates the frontal position of the glacier in 2017. Background image is a hillshade of the LiDAR DEM of Iceland from 2016. [Colour figure can be viewed at wileyonlinelibrary.com]

following the LIA, once Jökulsárlón increased to a sufficient size and was able to start influencing frontal retreat and ice flow, we suggest that this then became the dominant mechanism in causing the rapid retreat and flow velocities observed at Breiðamerkurjökull since the turn of the 21st century. This supports previous work that argues that the rapid retreat and highly dynamic changes occurring at calving glaciers cannot be solely attributed to climatic forcing alone, and, in exceptional cases, occurs completely independent of climatic influences (e.g. Meier and Post, 1987; Rignot *et al.*, 2003; Benn *et al.*, 2007a; Howat *et al.*, 2007; Sugiyama *et al.*, 2011; Sakakibara and Sugiyama, 2014).

We can contrast the behaviour of the eastern arm, with its rapid velocity and retreat rate, with the much slower and more stable western A arm, despite the presence of Breiðárlón at its margin. The area of Breiðárlón has remained approximately constant over our research period (Figures 6 and 7). We suggest that this stability is due to the topography of the bed. Beneath western A there is a much shallower trough (Figure 1), which sits above sea level for much of this distance (Guðmundsson *et al.*, 2017), while the depth of the lake itself is only thought to be approximately 60 m (Howarth and Price, 1967). Furthermore, the margin in this area is being pinned by large areas of bedrock (Schomacker, 2010) which are being exposed as the glacier retreats (Evans and Twigg, 2002). As a result, the lake has remained a similar depth, and the calving rate has remained relatively constant (Nick *et al.*, 2007), resulting in a more stable ice margin.

Implications and wider importance

The findings of this study show how soft-bedded, reverse-sloped, aquatic terminating glaciers in both Iceland and elsewhere may respond to future climate warming. In Iceland, widespread glacier retreat caused by climate warming has been occurring since 1985 (Sigurðsson, 1998; Sigurðsson *et al.*, 2007; Björnsson and Pálsson, 2008), and this rate of retreat has accelerated over recent years due to high summer melt forced by a 1 °C increase in mean annual temperature since the turn of the century (Björnsson and Pálsson, 2008; Jones *et al.*, 2012). The southern outlets of Vatnajökull, which have retreated rapidly since 1890, are particularly vulnerable to such warming conditions (Hannesdóttir *et al.*, 2015). This is because many carved deep subglacial troughs in the underlying soft sediments during their LIA advance, and consequently now have beds that sit 100–300 m at their deepest below the current elevation of the terminus (Björnsson *et al.*, 2001; Björnsson and Pálsson, 2008; Magnússon *et al.*, 2012). Now, as they rapidly retreat into these deep troughs, meltwater can infill the newly exposed topographic depressions, leading to the formation of proglacial lakes at their termini (Schomacker, 2010; Carrivick and Tweed, 2013). These lakes cause additional melting and mass loss through calving, facilitating further retreat and, therefore, further lake growth, initiating a positive feedback mechanism (Carrivick and Tweed, 2013; Hannesdóttir *et al.*, 2015).

As we have shown, such a feedback mechanism has been occurring at Breiðamerkurjökull since the mid-2000s, and as a

result there is the strong possibility that other southern outlets of Vatnajökull will undergo a similar pattern of retreat and mass loss in future (Schomacker, 2010; Dell *et al.*, 2019). For example, particularly deep troughs exist under the neighbouring outlets Svínafellsjökull (~320m), Skaftafellsjökull (230m) and Fjallsjökull (210m), and all have been undergoing rapid retreat since the 2000s (Magnússon *et al.*, 2012). Indeed, at Fjallsjökull, the adjacent glacier to Breiðamerkurjökull, such a mechanism is already thought to be underway (Magnússon *et al.*, 2012; Dell *et al.*, 2019).

Similar patterns of flow acceleration and retreat linked to increases in water depth have been observed at aquatic-terminating glaciers in other glaciated regions. For example, Brown *et al.* (1982) and Pelto and Warren (1991) found a strong relationship between an increase in water depth and an increase in calving speed for several Alaskan tidewater glaciers. At Mendenhall Glacier, Alaska, Motyka *et al.* (2003) found that as the glacier thinned and retreated into deeper water, the terminus reached floatation and destabilized. Once this occurred, the terminus began to calve at an increased rate into its proglacial lake, causing the glacier to retreat further into deeper water and initiating a positive feedback mechanism (Motyka *et al.*, 2003). Nick *et al.* (2009), in their study of Helheim Glacier in Greenland, successfully modelled the rapid acceleration (to 12 km year^{-1}) and thinning (>100m in 2 years) of the glacier as it retreated down its reverse-bed slope into deeper water. The retreat of the glacier over a bedrock high and back into deeper water caused ice speed and discharge to increase, leading to further thinning, retreat and the initiation of a positive feedback mechanism (Nick *et al.*, 2009). Finally, Sakakibara *et al.* (2013) attributed the observed recession and acceleration at Glacier Upsala, Patagonia to a change in the longitudinal stress exerted by the bed in response to the glacier retreating over a bedrock rise and down a reversed slope into deeper water.

Although there are differences between the processes influencing aquatic-terminating glaciers in these regions and those occurring on lake-terminating glaciers in Iceland, there are many similarities in their overall dynamics which could be the focus of future investigations at Breiðamerkurjökull. For example, the velocity time series could be extended back to 1982 to coincide with the period covered by our lake area and frontal position change data. The temporal gap between our velocity measurements could also be decreased (depending on data availability), which would allow us to investigate how the velocity of Breiðamerkurjökull varies over annual time scales. Finally, we could also extend the period covered by our surface elevation change analyses to match that of our other data series. This would allow for a more detailed comparison to be made between glacier dynamics, bedrock topography, surface thinning and lake depth. As a result, a more thorough understanding of the mechanisms and interactions occurring at Breiðamerkurjökull may help us to predict the response of these larger, more dynamic aquatic-terminating glaciers to climate change (e.g. Joughin *et al.*, 2012; Enderlin *et al.*, 2014).

Conclusions

We have presented the first multi-year, highly detailed velocity analyses of Breiðamerkurjökull, Iceland, covering almost three decades, using high-resolution SAR offset-tracking techniques. Our data demonstrate that the greatest retreat and increase in surface velocities is found for the larger, more dynamic eastern arm, with ~3.50km of recession (92.69 m year^{-1}) since 1982 and velocity increases occurring from ~2008 up to 2015, with values of up to 3.50 ±0.25 m day^{-1} recorded in the near-terminus region in 2015. This is in stark comparison to the other three arms, which see considerably less retreat (between ~1 and 2km), and where we do not detect any change in velocity beyond the uncertainty of our methods. We also observe a substantial increase in the area of Jökulsárlón since 1982 of ~20km^2, equating to an annual growth of 0.55 km^2 year^{-1}. We suggest that the differences between the eastern and other arms are due to the growth and, importantly, depth increase of Jökulsárlón as the eastern arm has retreated into the deep reverse-sloping subglacial trough it carved during the LIA. This triggered an increase in ice flow at the terminus due to the inverse relationship that exists between effective pressure and basal drag, leading to an increase in terminus retreat. Retreat down this reverse slope caused the water depth to increase further, initiating a positive feedback mechanism. As our results indicate, such feedback mechanisms are likely to be important for the future response of the other outlet glaciers in Iceland. As warming continues, these glaciers will retreat into their own subglacial troughs while lake development at their termini increases *in situ*, causing them to undergo a similar dynamic response to what we observe for Breiðamerkurjökull in this study. Our findings are also in agreement with the results of previous studies in other glaciated regions, which have investigated the link between flow speed, water depth and retreat, and therefore may give an indication of how the larger, soft-bedded, reverse-sloped, aquatic-terminating glaciers in other glaciated regions may respond in future.

Acknowledgements—The authors acknowledge the comments of two anonymous reviewers which greatly improved the quality of the manuscript. NB acknowledges the use of a virtual desktop machine provided by Copernicus Research User Support (RUS), which was utilized to process all SAR imagery. Thanks to the German AeroSpace Centre for the provision of the TerraSAR-X imagery and ESA for access to the ERS-1/2 and Sentinel data. Thanks also to USGS for the Landsat imagery, the National Land Survey of Iceland for the historic aerial photos and the Polar Geospatial Centre for use of the ArcticDEM.

Conflict of Interest

The authors declare no conflict of interest in the creation of this research paper.

Data Availability Statement

The Arctic DEM and LiDAR DEM of Iceland are available from https://www.pgc.umn.edu/data/arcticdem and https://gatt.lmi.is/geonetwork/srv/eng/catalog.search#/metadata/cb84d208-1b91-4b9e-a21c-93c4e284f488, respectively. The Sentinel and ERS data are available from the ESA, TerraSAR-X from DLR, Landsat from USGS and the archive aerial photographs from the National Land Survey of Iceland. Velocity rasters and surface elevation change data available on request from NRB (nrb1n18@soton.ac.uk).

References

Adhikari S, Marshall SJ. 2012. Parameterization of lateral drag in flowline models of glacier dynamics. *Journal of Glaciology* **58**(212): 1119–1132. https://doi.org/10.3189/2012JoG12J018

Andrews LC, Catania GA, Hoffman MJ, Gulley JD, Lüthi MP, Ryser C, Hawley RL, Neumann TA. 2014. Direct observations of evolving subglacial drainage beneath the Greenland Ice Sheet. *Nature* **514**(7520): 80–83. https://doi.org/10.1038/nature13796

Barr I, Dokukin M, Kougkoulos I, Livingstone S, Lovell H, Małecki J, Muraviev A. 2018. Using ArcticDEM to analyse the dimensions and dynamics of debris-covered glaciers in Kamchatka, Russia. *Geosciences* **8**(6): 216–233. https://doi.org/10.3390/geosciences8060216

Bartholomew ID, Nienow P, Sole A, Mair D, Cowton T, King MA, Palmer S. 2011. Seasonal variations in Greenland Ice Sheet motion: inland extent and behaviour at higher elevations. *Earth and Planetary Science Letters* **307**(3–4): 271–278. https://doi.org/10.1016/j.epsl.2011.04.014

Bartholomew I, Nienow P, Sole A, Mair D, Cowton T, King MA. 2012. Short-term variability in Greenland Ice Sheet motion forced by time-varying meltwater drainage: implications for the relationship between subglacial drainage system behaviour and ice velocity. *Journal of Geophysical Research: Earth Surface* **117**(F3), –. https://doi.org/10.1029/2011JF002220

Benn DI, Hulton NR, Mottram RH. 2007a. 'Calving laws', 'sliding laws' and the stability of tidewater glaciers. *Annals of Glaciology* **46**: 123–130. https://doi.org/10.3189/172756407782871161

Benn DI, Warren CR, Mottram RH. 2007b. Calving processes and the dynamics of calving glaciers. *Earth-Science Reviews* **82**(3–4): 143–179. https://doi.org/10.1016/j.earscirev.2007.02.002

Björnsson H. 1996. Scales and rates of glacial sediment removal: a 20 km long, 300 m deep trench created beneath Breiðamerkurjökull during the Little Ice Age. *Annals of Glaciology* **22**: 141–146. https://doi.org/10.3189/1996AoG22-1-141-146

Björnsson H, Pálsson F, Guðmundsson S. 2001. Jökulsárlón at Breiðamerkursandur, Vatnajökull, Iceland: 20th century changes and future outlook. *Jökull* **50**: 1–18.

Björnsson H, Pálsson F. 2008. Icelandic glaciers. *Jökull* **58**: 365–386.

Björnsson H, Pálsson F, Guðmundsson S, Magnússon E, Adalgeirsdóttir G, Jóhannesson T, Berthier E, Sigurðsson O, Thorsteinsson T. 2013. Contribution of Icelandic ice caps to sea level rise: trends and variability since the Little Ice Age. *Geophysical Research Letters* **40**(8): 1546–1550. https://doi.org/10.1002/grl.50278

Boulton GS, Dobbie KE, Zatsepin S. 2001. Sediment deformation beneath glaciers and its coupling to the subglacial hydraulic system. *Quaternary International* **86**(1): 3–28. https://doi.org/10.1016/S1040-6182(01)00048-9

Bradwell T, Sigurðsson O, Everest J. 2013. Recent, very rapid retreat of a temperate glacier in SE Iceland. *Boreas* **42**(4): 959–973. https://doi.org/10.1111/bor.12014

Brown CS, Meier MF, Post A. 1982. Calving speed of Alaska tidewater glaciers, with application to Columbia Glacier. *U.S. Geological Survey Professional Paper* **1258**(C): 1–13.

Carrivick JL, Tweed FS. 2013. Proglacial lakes: character, behaviour and geological importance. *Quaternary Science Reviews* **78**: 34–52. https://doi.org/10.1016/j.quascirev.2013.07.028

Cazenave A, WCRP Global Sea Level Budget Group. 2018. Global sea-level budget 1993–present. *Earth System Science Data* **10**: 1551–1590. https://doi.org/10.3929/ethz-b-000287786

Cowton T, Nienow P, Sole A, Wadham J, Lis G, Bartholomew I, Mair D, Chandler D. 2013. Evolution of drainage system morphology at a land-terminating Greenlandic outlet glacier. *Journal of Geophysical Research: Earth Surface* **118**(1): 29–41. https://doi.org/10.1029/2012JF002540

Cuffey KH, Paterson WSB. 2010. *The Physics of Glaciers*, 4th edn. Elsevier: Burlington, VA.

Dehecq A, Gourmelen N, Trouvé E. 2015. Deriving large-scale glacier velocities from a complete satellite archive: application to the Pamir–Karakoram–Himalaya. *Remote Sensing of Environment* **162**: 55–66. https://doi.org/10.1016/j.rse.2015.01.031

Dehecq A, Gourmelen N, Gardner AS, Brun F, Goldberg D, Nienow PW, Berthier E, Vincent C, Wagnon P, Trouvé E. 2019. Twenty-first century glacier slowdown driven by mass loss in High Mountain Asia. *Nature Geoscience* **12**: 22–27. https://doi.org/10.1038/s41561-018-0271-9

Dell R, Carr R, Phillips E, Russell AJ. 2019. Response of glacier flow and structure to proglacial lake development and climate at Fjallsjökull, south-east Iceland. *Journal of Glaciology* **65**(250): 321–336. https://doi.org/10.1017/jog.2019.18

Einarsson B. 2017. Jöklabreytingar 1930–1970, 1970–1995, 1995–2015 & 2015–2016. *Jökull* **67**: 65–69.

Enderlin EM, Howat IM, Jeong S, Noh MJ, van Angelen JH, van den Broeke MR. 2014. An improved mass budget for the Greenland ice sheet. *Geophysical Research Letters* **41**(3): 866–872 https://doi.org/10.1002/2013GL059010

ESA. 2016. SNAP Sentinel-1 toolbox [Software and support]. Retrieved from http://step.esa.int/main/download/

Evans DJ, Twigg DR. 2002. The active temperate glacial landsystem: a model based on Breiðamerkurjökull and Fjallsjökull, Iceland. *Quaternary Science Reviews* **21**(20–22): 2143–2177. https://doi.org/10.1016/S0277-3791(02)00019-7

Fahnestock M, Scambos T, Moon T, Gardner A, Haran T, Klinger M. 2016. Rapid large-area mapping of ice flow using Landsat 8. *Remote Sensing of Environment* **185**: 84–94. https://doi.org/10.1016/j.rse.2015.11.023

Flowers GE, Marshall SJ, Björnsson H, Clarke GK. 2005. Sensitivity of Vatnajökull ice cap hydrology and dynamics to climate warming over the next 2 centuries. *Journal of Geophysical Research: Earth Surface* **110**(F2). https://doi.org/10.1029/2004JF000200

Foresta L, Gourmelen N, Pálsson F, Nienow P, Björnsson H, Shepherd A. 2016. Surface elevation change and mass balance of Icelandic ice caps derived from swath mode CryoSat-2 altimetry. *Geophysical Research Letters* **43**(23). https://doi.org/10.1002/2016GL071485

Gjermundsen EF, Mathieu R, Kääb A, Chinn T, Fitzharris B, Hagen JO. 2011. Assessment of multispectral glacier mapping methods and derivation of glacier area changes, 1978–2002, in the central Southern Alps, New Zealand, from ASTER satellite data, field survey and existing inventory data. *Journal of Glaciology* **57**(204): 667–683. https://doi.org/10.3189/002214311797409749

Glasser NF, Holt TO, Evans ZD, Davies BJ, Pelto M, Harrison S. 2016. Recent spatial and temporal variations in debris cover on Patagonian glaciers. *Geomorphology* **273**: 202–216. https://doi.org/10.1016/j.geomorph.2016.07.036

Guðmundsson S, Björnsson H. 2016. Changes in the flow pattern of Breiðamerkurjökull reflected by bending of the Esjufjallarond medial moraine. *Jökull* **66**: 95–100.

Guðmundsson S, Björnsson H, Pálsson F. 2017. Changes of Breiðamerkurjökull glacier, SE-Iceland, from its late nineteenth century maximum to the present. *Geografiska Annaler: Series A, Physical Geography* **99**(4): 338–352. https://doi.org/10.1080/04353676.2017.1355216

Haeberli W, Buetler M, Huggel C, Friedli TL, Schaub Y, Schleiss AJ. 2016. New lakes in deglaciating high-mountain regions – opportunities and risks. *Climatic Change* **139**(2): 201–214. https://doi.org/10.1007/s10584-016-1771-5

Hannesdóttir H, Björnsson H, Pálsson F, Aðalgeirsdóttir G, Guðmundsson S. 2015. Changes in the southeast Vatnajökull ice cap, Iceland, between ~1890 and 2010. *The Cryosphere* **9**(2): 565–585. https://doi.org/10.5194/tc-9-565-2015

Hart JK, Rose KC, Waller RI, Vaughan-Hirsch D, Martinez K. 2011. Assessing the catastrophic break-up of Briksdalsbreen, Norway, associated with rapid climate change. *Journal of the Geological Society* **168**(3): 673–688. https://doi.org/10.1144/0016-76492010-024

Hart JK, Martinez K, Basford PJ, Clayton AI, Bragg GM, Ward T, Young DS. 2019a. Surface melt-driven seasonal behaviour (englacial and subglacial) from a soft-bedded temperate glacier recorded by in situ wireless probes. *Earth Surface Processes and Landforms* **44**(9): 1769–1782. https://doi.org/10.1002/esp.4611

Hart JK, Martinez K, Basford PJ, Clayton AI, Robson BA, Young DS. 2019b. Surface melt driven summer diurnal and winter multi-day stick-slip motion and till sedimentology. *Nature Communications* **10**(1). https://doi.org/10.1038/s41467-019-09547-6

Heid T, Kääb A. 2012. Repeat optical satellite images reveal widespread and long term decrease in land-terminating glacier speeds. *The Cryosphere* **6**: 467–478. https://doi.org/10.5194/tc-6-467-2012

Howarth PJ, Price RJ. 1967. The proglacial lakes of Breiðamerkurjökull and Fjallsjökull, Iceland. *The Geographical Journal* **135**(4): 573–581. https://doi.org/10.2307/1795105

Howat IM, Joughin I, Tulaczyk S, Gogineni S. 2005. Rapid retreat and acceleration of Helheim Glacier, east Greenland. *Geophysical Research Letters* **32**(22). https://doi.org/10.1029/2005GL024737

Howat IM, Joughin I, Scambos TA. 2007. Rapid changes in ice discharge from Greenland outlet glaciers. *Science* **315**(5818): 1559–1561. https://doi.org/10.1126/science.1138478

Howat IM, Tulaczyk S, Waddington E, Björnsson H. 2008. Dynamic controls on glacier basal motion inferred from surface ice motion. *Journal of Geophysical Research: Earth Surface* **113**(F3). https://doi.org/10.1029/2007JF000925

Howat IM, Eddy A. 2011. Multi-decadal retreat of Greenland's marine-terminating glaciers. *Journal of Glaciology* **57**(203): 389–396. https://doi.org/10.3189/002214311796905631

Huss M, Hock R. 2015. A new model for global glacier change and sea-level rise. *Frontiers in Earth Science* **3**: 54. https://doi.org/10.3389/feart.2015.00054

Huss M, Hock R. 2018. Global-scale hydrological response to future glacier mass loss. *Nature Climate Change* **8**(2): 135–140. https://doi.org/10.1038/s41558-017-0049-x

Immerzeel WW, Kraaijenbrink PDA, Shea JM, Shrestha AB, Pellicciotti F, Bierkens MFP, de Jong SM. 2014. High-resolution monitoring of Himalayan glacier dynamics using unmanned aerial vehicles. *Remote Sensing of Environment* **150**: 93–103. https://doi.org/10.1016/j.rse.2014.04.025

Jones PD, Lister DH, Osborn TJ, Harpham C, Salmon M, Morice CP. 2012. Hemispheric and large-scale land-surface air temperature variations: an extensive revision and an update to 2010. *Journal of Geophysical Research: Atmospheres* **117**(D5). https://doi.org/10.1029/2011JD017139

Joughin I, Smith BE, Howat IM, Floricioiu D, Alley RB, Truffer M, Fahnestock M. 2012. Seasonal to decadal scale variations in the surface velocity of Jakobshavn Isbrae, Greenland: observation and model-based analysis. *Journal of Geophysical Research: Earth Surface* **117**(F2). https://doi.org/10.1029/2011JF002110

Joughin I, Smith BE, Howat I. 2018. Greenland Ice Mapping Project: ice flow velocity variation at sub-monthly to decadal time scales. *The Cryosphere* **12**(7): 2211–2227. https://doi.org/10.5194/tc-12-2211-2018

King O, Dehecq A, Quincey D, Carrivik J. 2018. Contrasting geometric and dynamic evolution of lake and land-terminating glaciers in the central Himalaya. *Global and Planetary Change* **167**: 46–60. https://doi.org/10.1016/j.gloplacha.2018.05.006

Larsen SH, Khan SA, Ahlstrøm AP, Hvidberg CS, Willis MJ, Andersen SB. 2016. Increased mass loss and asynchronous behaviour of marine-terminating outlet glaciers at Upernavik Isstrøm, NW Greenland. *Journal of Geophysical Research: Earth Surface* **121**(2): 241–256. https://doi.org/10.1002/2015JF003507

Lea JM, Mair DW, Rea BR. 2014. Evaluation of existing and new methods of tracking glacier terminus change. *Journal of Glaciology* **60**(220): 241–256. https://doi.org/10.3189/2014JoG13J061

Lovell A. 2016. The drivers of inter-annual outlet glacier terminus change in Victoria Land, Oates Land and George V Land, East Antarctica (1972–2013). PhD thesis, Durham University. Retrieved from http://etheses.dur.ac.uk/11561

Lu J, Veci L. 2016. Sentinel-1 Toolbox: offset tracking tutorial. Retrieved from http://step.esa.int/docs/tutorials/S1TBX%20Offset%20Tracking%20Tutorial.pdf

Magnússon E, Pálsson F, Björnsson H, Guðmundsson S. 2012. Removing the ice cap of Öræfajökull central volcano, SE Iceland: mapping and interpretation of bedrock topography, ice volumes, subglacial troughs and implications for hazards assessments. *Jökull* **62**: 131–150.

Meier MF, Post A. 1987. Fast tidewater glaciers. *Journal of Geophysical Research: Solid Earth* **92**(B9): 9051–9058. https://doi.org/10.1029/JB092iB09p09051

Mernild SH, Knudsen NT, Hoffman MJ, Yde JC, Hanna E, Lipscomb WH, Malmros JK, Fausto RS. 2013. Volume and velocity changes at Mittivakkat Gletscher, southeast Greenland. *Journal of Glaciology* **59**(216): 660–670. https://doi.org/10.3189/2013JoG13J017

Moon T, Joughin I. 2008. Changes in ice front position on Greenland's outlet glaciers from 1992 to 2007. *Journal of Geophysical Research: Earth Surface* **113**(F2). https://doi.org/10.1029/2007JF000927

Morin P, Porter C, Cloutier M, Howat I, Noh MJ, Willis M, Bates B, Willamson C, Peterman K. 2016. ArcticDEM; a publicly available, high resolution elevation model of the Arctic. *In EGU General Assembly Conference Abstracts* **18**.

Motyka RJ, O'Neel S, Connor CL, Echelmeyer KA. 2003. Twentieth century thinning of Mendenhall Glacier, Alaska, and its relationship to climate, lake calving and glacier run-off. *Global and Planetary Change* **35**(1–2): 92–112. https://doi.org/10.1016/S0921-8181(02)00138-8

Nagler T, Rott H, Hetzenecker M, Scharrer K, Magnússon E, Floricioiu D, Notarnicola C. 2012. In 2012 IEEE International Geoscience and Remote Sensing Symposium (pp. 3233–3236). https://doi.org/10.1109/IGARSS.2012.6350735

Nagler T, Rott H, Hetzenecker M, Wuite J, Potin P. 2015. The Sentinel-1 mission: new opportunities for ice sheet observations. *Remote Sensing* **7**(7): 9371–9389. https://doi.org/10.3390/rs70709371

Naruse R, Skvarca P. 2000. Dynamic features of thinning and retreating Glaciar Upsala, a lacustrine calving glacier in southern Patagonia. *Arctic, Antarctic, and Alpine Research* **32**(4): 485–491 https://doi.org/10.1080/15230430.2000.12003393

Nick FM, Van der Kwast J, Oerlemans J. 2007. Simulation of the evolution of Breidamerkurjökull in the late Holocene. *Journal of Geophysical Research: Solid Earth* **112**(B1). https://doi.org/10.1029/2006JB004358

Nick FM, Vieli A, Howat IM, Joughin I. 2009. Large-scale changes in Greenland outlet glacier dynamics triggered at the terminus. *Nature Geoscience* **2**: 110–114. https://doi.org/10.1038/ngeo394

Nie Y, Sheng Y, Liu Q, Liu L, Liu S, Zhang Y, Song C. 2017. A regional-scale assessment of Himalayan glacial lake changes using satellite observations from 1990 to 2015. *Remote Sensing of Environment* **189**: 1–13. https://doi.org/10.1016/j.rse.2016.11.008

Nuth C, Kääb A. 2011. Co-registration and bias corrections of satellite elevation data sets for quantifying glacier thickness change. *The Cryosphere* **5**(1): 271–290. https://doi.org/10.5194/tc-5-271-2011

Nuth C, Schuler TV, Kohler J, Altena B, Hagen JO. 2012. Estimating the long-term calving flux of Kronebreen, Svalbard, from geodetic elevation changes and mass-balance modelling. *Journal of Glaciology* **58**(207): 119–133. https://doi.org/10.3189/2012JoG11J036

Pelto MS, Warren CR. 1991. Relationship between tidewater glacier calving velocity and water depth at the calving front. *Annals of Glaciology* **15**: 115–118. https://doi.org/10.3189/S0260305500009617

Pritchard HD, Arthern RJ, Vaughan DG, Edwards LA. 2009. Extensive dynamic thinning on the margins of the Greenland and Antarctic ice sheets. *Nature* **461**(7266): 971–975. https://doi.org/10.1038/nature08471

Racoviteanu AE, Paul F, Raup B, Khalsa SJS, Armstrong R. 2009. Challenges and recommendations in mapping glacier parameters from space: results of the 2008 Global Land Ice Measurements from Space (GLIMS) workshop, Boulder, Colorado, USA. *Annals of Glaciology* **50**(53): 53–69. https://doi.org/10.3189/172756410790595804

Rignot E, Rivera A, Casassa G. 2003. Contribution of the Patagonia Icefields of South America to sea level rise. *Science* **302**(5644): 434–437. https://doi.org/10.1126/science.1087393

Robson BA, Nuth C, Nielsen PR, Girod L, Hendrickx M, Dahl SO. 2018. Spatial variability in patterns of glacier change across the Manaslu Range, Central Himalaya. *Frontiers in Earth Science* **6**: 1–12. https://doi.org/10.3389/feart.2018.00012

Rossini M, Di Mauro B, Garzonio R, Baccolo G, Cavallini G, Mattavelli M, De Amicis M, Colombo R. 2018. Rapid melting dynamics of an alpine glacier with repeated UAV photogrammetry. *Geomorphology* **304**: 159–172. https://doi.org/10.1016/j.geomorph.2017.12.039

Röthilsberger H. 1972. Water pressure in intra- and subglacial channels. *Journal of Glaciology* **11**(62): 177–203. https://doi.org/10.3189/S0022143000022188

Sakakibara D, Sugiyama S, Sawagaki T, Marinsek S, Skvarca P. 2013. Rapid retreat, acceleration and thinning of Glaciar Upsala, Southern Patagonia Icefield, initiated in 2008. *Annals of Glaciology* **54**(63): 131–138. https://doi.org/10.3189/2013AoG63A236

Sakakibara D, Sugiyama S. 2014. Ice-front variations and speed changes of calving glaciers in the Southern Patagonia Icefield from 1984 to 2011. *Journal of Geophysical Research: Earth Surface* **119**(11): 2541–2554. https://doi.org/10.1002/2014JF003148

Schomacker A. 2010. Expansion of ice-marginal lakes at the Vatnajökull ice cap, Iceland, from 1999 to 2009. *Geomorphology* **119**(3–4): 232–236. https://doi.org/10.1016/j.geomorph.2010.03.022

Schoof C. 2010. Ice-sheet acceleration driven by melt supply variability. *Nature* **468**(7325): 803–806. https://doi.org/10.1038/nature09618

Serco Italia SPA. 2018. Glacier velocity with Sentinel-1 – Peterman Glacier, Greenland. [Offset Tracking Tutorial, V.1.2]. Retrieved from https://rus-copernicus.eu/portal/the-rus-library/learn-by-yourself/

Shannon S, Smith R, Wiltshire A, Payne T, Huss M, Betts R, Caesar J, Koutroulis A, Jones D, Harrison S. 2019. Global glacier volume projections under high-end climate change scenarios. *The Cryosphere* **13**: 325–350. https://doi.org/10.5194/tc-13-325-2019

Sigurđsson O. 1998. Glacier variations in Iceland 1930–1995 – from the database of the Icelandic Glaciological Society. *Jökull* **45**: 3–25.

Sigurđsson O, Jonsson T, Johannesson T. 2007. Relation between glacier-termini variations and summer temperature in Iceland since 1930. *Annals of Glaciology* **46**: 170–176. https://doi.org/10.3189/172756407782871611

Staines KEH, Carrivick JL, Tweed FS, Evans AJ, Russel AJ, Jóhannesson T, Roberts M. 2015. A multi-dimensional analysis of pro-glacial landscape change at Sólheimajökull, southern Iceland. *Earth Surface Processes and Landforms* **40**(6): 809–822. https://doi.org/10.1002/esp.3662

Storrar RD, Jones AH, Evans DJ. 2017. Small-scale topographically controlled glacier flow switching in an expanding proglacial lake at Breiðamerkurjökull, SE Iceland. *Journal of Glaciology* **63**(240): 745–750. https://doi.org/10.1017/jog.2017.22

Sugiyama S, Skvarca P, Naito N, Enomoto H, Tsutaki S, Tone K, Marinsek S, Aniya M. 2011. Ice speed of a calving glacier modulated by small fluctuations in basal water pressure. *Nature Geoscience* **4** (9): 597–600. https://doi.org/10.1038/ngeo1218

Tedstone AJ, Nienow PW, Sole AJ, Mair DWF, Cowton TR, Bartholomew ID, King MA. 2013. Greenland ice sheet motion insensitive to exceptional meltwater forcing. *Proceedings of the National Academy of Sciences* **110**(49): 19719–19724. https://doi.org/10.1073/pnas.1315843110

Tedstone AJ, Nienow PW, Gourmelen N, Dehecq A, Goldberg D, Hanna E. 2015. Decadal slowdown of a land-terminating sector of the Greenland Ice Sheet despite warming. *Nature* **526**: 692–695. https://doi.org/10.1038/nature15722

Van der Veen CJ. 2002. Calving glaciers. *Progress in Physical Geography* **26**(1): 96–122. https://doi.org/10.1191/2F0309133302pp327ra

Voytenko D, Dixon TH, Howat IM, Gourmelen N, Lembke C, Werner CL, De La Peña S, Oddsson B. 2015. Multi-year observations of Breiðamerkurjökull, a marine-terminating glacier in southeastern Iceland, using terrestrial radar interferometry. *Journal of Glaciology* **61**(225): 42–54. https://doi.org/10.3189/2015JoG14J099

Warren CR, Kirkbride MP. 2003. Calving speed and climatic sensitivity of New Zealand lake-calving glaciers. *Annals of Glaciology* **36**: 173–178. https://doi.org/10.3189/172756403781816446

Zemp M, Frey H, Gärtner-Roer I, Nussbaumer SU, Hoelzle M, Paul F, Haeberli W, Denzinger F, Ahlstrøm AP, Anderson B, Bajracharya S, Baroni C, Braun LN, Cáceres BE, Casassa G, Cobos G, Dávila LR, Delgado Granados H, Demuth MN, Espizua L, Fischer A, Fujita K, Gadek B, Ghazanfar A, Hagen JO, Holmlund P, Karimi N, Li Z, Pelto M, Pitte P, Popovnin VV, Portocarrero CA, Prinz R, Sangewar V, Severskiy I, Sigurđsson O, Soruco A, Usubaliev R, Vincent C. 2015. Historically unprecedented global glacier changes in the early 21st century. *Journal of Glaciology* **61**(228): 745–762. https://doi.org/10.3189/2015JoG15J017

Zemp M, Huss M, Thibert E, Eckert N, McNabb R, Huber J, Barandun M, Machguth H, Nussbaumer SU, Gärtner-Roer I, Thomson L, Paul F, Maussion F, Kutuzov S, Cogley JJ. 2019. Global glacier mass changes and their contributions to sea-level rise from 1961 to 2016. *Nature* **568**(7752): 382–386. https://doi.org/10.1038/s41586-019-1071-0

Zhang G, Bolch T, Allen S, Linsbauer A, Chen W, Wang W. 2019. Glacial lake evolution and glacier–lake interactions in the Poiqu River basin, central Himalaya, 1964–2017. *Journal of Glaciology* **65** (251): 347–365. https://doi.org/10.1017/jog.2019.13

Zwally HJ, Abdalati W, Herring T, Larson K, Saba J, Steffen K. 2002. Surface melt-induced acceleration of Greenland ice-sheet flow. *Science* **297**(5579): 218–222. https://doi.org/10.1126/science.1072708

Landmælingar Íslands. 2016. National Land Survey of Iceland – LiDAR DEM of Iceland. Retrieved from https://gatt.lmi.is/geonetwork/srv/eng/catalog.search#/metadata/cb84d208-1b91-4b9e-a21c-93c4e284f488

Porter C, Morin P, Howat I, Noh M-J, Bates B, Peterman K, Keesey S, Schlenk M, Gardiner J, Tomko K, Willis M, Kelleher C, Cloutier M, Husby E, Foga S, Nakamura H, Platson M, Wethington M Jr, Williamson C, Bauer G, Enos J, Arnold G, Kramer W, Becker P, Doshi A, D'Souza C, Cummens P, Laurier F, Bojesen M. 2018. Arctic DEM. Harvard Dataverse V1. Retrieved from https://www.pgc.umn.edu/data/arcticdem/

MeierbachtolT., Harper J., Humphrey N. (2013) Basal Drainage System Response to Increasing Surface Melt on the Greenland Ice Sheet. *Science*, **341** (6147), 777–779. https://doi.org/10.1126/science.1235905.

SoleA, Nienow P, Bartholomew I, Mair D, Cowton T, Tedstone A, King MA. (2013) Winter motion mediates dynamic response of the Greenland Ice Sheet to warmer summers. *Geophysical Research Letters*, **40** (15), 3940–3944. https://doi.org/10.1002/grl.50764.

BougamontM, Christoffersen P, Hubbard AL, Fitzpatrick AA, Doyle SH, Carter SP. (2014) Sensitive response of the Greenland Ice Sheet to surface melt drainage over a soft bed. *Nature Communications*, **5** (1), https://doi.org/10.1038/ncomms6052.

Supporting Information

Additional supporting information may be found online in the Supporting Information section at the end of the article.

Figure S1. SNAP-obtained velocity outputs for all years covering our study period. All outputs shown at 20% transparency overlaid on a hillshade of the LiDAR DEM of Iceland from 2016. Longitudinal flowlines are also shown. Glacier outlines (white) and lake areas (light green) are from each respective year.

Figure S2. Velocity profiles for the eastern arm of Breiðamerkurjökull for the period 1991–2018, calculated by taking the mean velocity at 1 km segments along the entire length of the central flowline. Associated uncertainty margins for each year are also shown.

Figure S3. Velocity profiles for the central arm of Breiðamerkurjökull for the period 1991–2018, calculated by taking the mean velocity at 1 km segments along the entire length of the central flowline. Associated uncertainty margins for each year are also shown.

Figure S4. Velocity profiles for the western 'A' arm of Breiðamerkurjökull for the period 1991–2018, calculated by taking the mean velocity at 1 km segments along the entire length of the central flowline. Associated uncertainty margins for each year are also shown.

Figure S5. Velocity profiles for the western 'B' arm of Breiðamerkurjökull for the period 1991–2018, calculated by taking the mean velocity at 1 km segments along the entire length of the central flowline. Associated uncertainty margins for each year are also shown.

